

# Testing LRD in the spectral domain for functional time series in manifolds

M.D. Ruiz–Medina<sup>1</sup>, R.M. Crujeiras<sup>2</sup>

<sup>1</sup> Department of Statistics and Operation Research, University of Granada

<sup>2</sup> Galician Center for Mathematical Research and Technology, CITMAga, Universidad de Santiago de Compostela

## Abstract

A statistical hypothesis test for long range dependence (LRD) in manifold–supported functional time series is formulated in the spectral domain. The proposed test statistic operator is based on the weighted periodogram operator. It is assumed that the elements of the spectral density operator family are invariant with respect to the group of isometries of the manifold. A Central Limit Theorem is derived to obtain the asymptotic Gaussian distribution of the proposed test statistics operator under the null hypothesis. The rate of convergence to zero, in the Hilbert–Schmidt operator norm, of the bias of the integrated empirical second and fourth order cumulant spectral density operators is established under the alternative hypothesis. The consistency of the test is derived, from the consistency, in the sense of the integrated mean square error, of the weighted periodogram operator under LRD. Our proposal to implement, in practice, the testing approach is based on the temporal–frequency–varying Karhunen–Loève expansion obtained here for invariant random Hilbert–Schmidt kernels on manifolds. A simulation study illustrates the main results regarding asymptotic normality and consistency, and the empirical size and power properties of the proposed testing approach.

*Keywords* Asymptotic normality, bias, compact manifolds, consistency, empirical cumulant spectral density operator, functional time series, integrated weighted periodogram operator, long-range dependence, spectral density operator.

# 1 Introduction

Spherical functional time series analysis helps in understanding the dynamics and spatiotemporal patterns of data that are embedded into the sphere, providing valuable insights for prediction, monitoring, and decision-making. Time series analysis of global temperature data distribution or other climate variables, usually arising in Climate Science and Meteorology, can be performed in a more efficient way by adopting a functional time series framework (see [29]). That is the case of ocean currents, and other marine functional time series to be analyzed in Oceanography studies (see, e.g., [32]; [34]). Other areas demanding this type of techniques are Geophysics, Astronomy and Astrophysics. In the last few decades, the cosmic microwave background radiation variation analysis over time has acquired special significance (see [2]; [3]; [16]; [15]). In a more general manifold setting, functional time series analysis is often applied in Medical Imaging, Computer Vision and Graphics (see [33]; [35]; [36], among others). This paper focuses on the spectral analysis of manifold-supported functional time series, paying special attention to LRD analysis.

The spectral analysis of functional time series has mainly been developed under Short Range Dependence (SRD). In this context, based on the weighted periodogram operator, a nonparametric framework is adopted in [20]. Particularly, the asymptotic normality of the functional discrete Fourier transform (fDFT), and the weighted periodogram operator of the curve data is proved under suitable summability conditions on the cumulant spectral density operators. The consistency of the weighted periodogram operator, in the sense of the integrated mean square error, as well as pointwise, in the Hilbert–Schmidt operator norm, is also derived under SRD. In [21], a harmonic principal component analysis of functional time series in the temporal functional spectral domain is derived, based on a Karhunen–Loève–like decomposition, the so-called Cramér–Karhunen–Loève representation (see also [26]; [27]). In the context of functional regression, some applications are presented in [22] and [30]. Hypothesis testing for detecting modelling differences in functional time series dynamics is addressed in [31] in the functional spectral domain.

Only a few contributions can be found on LRD functional time series analysis. One of the key approaches in the current literature is presented in [13], where the eigendecomposition of the long-run covariance operator is considered, under an asymptotic semiparametric functional principal component framework. The consistent estimation of the dimension and the orthonormal functions spanning the dominant subspace, where the projected curve process displays the largest dependence range is derived. Fractionally integrated functional autoregressive moving averages processes constitute an interesting example of this modelling framework.

A first attempt to characterize LRD in functional time series in the spectral domain can be found in [28], adopting the theoretical framework of operator-valued random fields, including fractional Brownian motion with operator-valued Hurst coefficient (see, e.g., [8], [9], [23], and [24]). Specifically, the LRD functional time series setting introduced in [28] in a semiparametric framework in the functional spectral domain is based on the consideration of a parameterized LRD operator. The eigenvalues of this operator induce different levels of singularity at zero frequency. Thus, different levels of LRD are displayed in time by the process projected into different eigenspaces. The asymptotic unbiasedness in the Hilbert–Schmidt operator norm of the integrated periodogram operator under LRD is proved beyond any structural assumptions. The weak-consistent minimum contrast estimation of the LRD operator is addressed in the temporal functional spectral domain under a Gaussian scenario. Interesting examples of this setting are analyzed in [18], where the spectral analysis of multifractionally integrated functional time series in manifolds is considered. In particular, multifractionally integrated spherical functional ARMA models (i.e., multifractionally integrated SPHARMA models) are analyzed through simulations. In this modelling framework, SRD and LRD can coexist at different spherical scales. See also [12] for the purely spatial case.

Up to our knowledge, no further developments have been achieved in the spectral analysis of LRD functional time series. In this paper we perform a weighted periodogram operator based analysis, requiring the asymptotic analysis of the bias of the integrated fourth-order empirical cumulant spectral density operators, to prove consistency of the integrated weighted periodogram operator under LRD. Its application to spectral statistical hypothesis testing of LRD in  $L^2(\mathbb{M}_d, d\nu, \mathbb{R})$ -valued correlated sequences constitutes one of the main goals of this work. Here,  $L^2(\mathbb{M}_d, d\nu, \mathbb{R})$  denotes the space of real-valued square integrable functions on a Riemannian manifold  $\mathbb{M}_d$ , given by a connected and compact two-point homogeneous space, with  $d$  denoting its topological dimension, and  $d\nu$  being the normalized Riemannian measure on  $\mathbb{M}_d$ . Manifold  $\mathbb{M}_d$  is assumed to be embedded into  $\mathbb{R}^{d+1}$ . In what follows, we will consider  $X = \{X_t, t \in \mathbb{Z}\}$  to be a functional sequence such that  $\mathcal{P}(X_t \in L^2(\mathbb{M}_d, d\nu, \mathbb{R})) = 1$ , for every  $t \in \mathbb{Z}$ , with  $\mathcal{P}$  denoting the probability measure defined on the basic probability space  $(\Omega, \mathcal{Q}, \mathcal{P})$ , i.e., for every  $t \in \mathbb{Z}$ ,

$$X_t : (\Omega, \mathcal{Q}, \mathcal{P}) \longrightarrow L^2(\mathbb{M}_d, d\nu, \mathbb{R}) \quad (1)$$

is a measurable mapping.

The invariance of the elements of the spectral density operator family of  $X$  under the group of isometries of the manifold  $\mathbb{M}_d$  is assumed along the paper. A frequency-varying eigenvalue sequence then characterizes the pure point spectra of the elements of the spectral density operator family, with respect to the

eigenfunctions of the Laplace–Beltrami operator. This assumption is exploited in the Central Limit Theorem derived here to characterize the asymptotic distribution of the proposed test statistics operator under the null hypothesis, which states that  $X$  displays SRD. In our formulation of the alternative hypothesis on LRD, we adopt a semiparametric framework in terms of a functional parameter given by the LRD operator. In contrast with the approach presented in [28], here we do not assume a parameterization of the eigenvalues of the LRD operator. Proposition 1 shows the divergence, in the Hilbert–Schmidt operator norm, of the mean of the test statistics operator under the alternative hypothesis. Theorem 2 derives suitable conditions on the nonparametric functional spectral factor to ensure consistency on the integrated weighted periodogram operator under LRD. Theorem 3 then provides the almost surely divergence of the test statistics in the Hilbert–Schmidt operator norm under the alternative, yielding the consistency of the test.

Theorem 3 also plays a crucial role in the implementation in practice of the proposed testing procedure, based on rejecting the null hypothesis when the Fourier coefficients of the test operator statistics, suitably standardized according to Lemma 4 and Theorem 1, cross an upper or lower tail standard normal critical value. The involved orthonormal basis is constructed by the tensorial product of the eigenfunctions of the Laplace Beltrami operator. The random projection methodology (see Theorem 4.1 in [5]) can be implemented here to alleviate the dimensionality problem. Specifically, when the moments of our test statistics operator satisfy the Carleman condition, our testing procedure is equivalent to rejecting the null hypothesis when the absolute value of a random projection of the test statistics is larger than an upper tail standard normal critical value. The Karhunen–Loève expansion derived in Lemma 4 below plays a crucial role in the generation of the Gaussian random directions required in the implementation of the random projection procedure. Furthermore, as illustrated in the simulation study undertaken, the empirical size properties of the proposed test procedure are quite robust, and competitive in terms of power (see Section 5.4 below).

The outline of the paper is the following. In Section 1.1, the functional spectral background material is introduced. Our hypothesis testing procedure is formulated in a semiparametric functional spectral framework in Section 1.2. The asymptotic Gaussian distribution of the test statistics operator under  $H_0$  is obtained in Theorem 1 in Section 2. Asymptotics of the bias of the integrated second and fourth order empirical cumulant spectral density operators under LRD are derived in Section 3. In Section 4, the preliminary results required for consistency, as well as Theorem 3, are established. In Section 5.1, a simulation study is undertaken to illustrate the asymptotic Gaussian distribution of the proposed test statistics operator under the null hypothesis, in the context of spherical functional time series. The consistency of this test is also illustrated in

Section 5.2, in the framework of multifractionally integrated spherical functional time series. Section 5.4 analyzes empirical size and power properties of the proposed test. Section 6 ends the paper with final comments, and discussion regarding the large functional sample size properties of the proposed test statistics operator under different bandwidth parameter scenarios, as well as beyond some structural restrictions arising in our LRD scenario under the alternative. The proofs of the results of this paper can be found in the Appendices. Also, Appendix D provides the figures illustrating Examples 1–4 in Sections 5.2–5.3.

## 1.1 Background

Along this work we will assume that  $X = \{X_t, t \in \mathbb{Z}\}$  in (1) is a stationary zero-mean functional sequence, and that its family of nuclear covariance operators  $\{\mathcal{R}_\tau, \tau \in \mathbb{Z}\}$  satisfies  $\mathcal{R}_\tau = E[X_s \otimes X_{s+\tau}] = E[X_{s+\tau} \otimes X_s]$ , for every  $s, \tau \in \mathbb{Z}$ . The elements of this family are characterized in the spectral domain by the spectral density operator family  $\{\mathcal{F}_\omega, \omega \in [-\pi, \pi]\}$ . The assumed invariance of the elements of these families with respect to the group of isometries of  $\mathbb{M}_d$  leads to their diagonal series expansion in terms of  $\{S_{n,j}^d \otimes S_{n,j}^d, j = 1, \dots, \Gamma(n, d), n \in \mathbb{N}_0\}$ , with  $\{S_{n,j}^d, j = 1, \dots, \Gamma(n, d), n \in \mathbb{N}_0\}$  being the eigenfunctions of the Laplace–Beltrami operator  $\Delta_d$  on  $L^2(\mathbb{M}_d, d\nu, \mathbb{R})$ . In particular,

$$\begin{aligned} \mathcal{F}_\omega & \underset{S(L^2(\mathbb{M}_d, d\nu; \mathbb{C}))}{=} \frac{1}{2\pi} \sum_{\tau \in \mathbb{Z}} \exp(-i\omega\tau) \mathcal{R}_\tau \\ & \underset{S(L^2(\mathbb{M}_d, d\nu; \mathbb{C}))}{=} \sum_{n \in \mathbb{N}_0} f_n(\omega) \sum_{j=1}^{\Gamma(n, d)} S_{n,j}^d \otimes S_{n,j}^d, \quad \omega \in [-\pi, \pi], \end{aligned} \quad (2)$$

where, for every  $n \in \mathbb{N}_0$ ,  $\Gamma(n, d)$  denotes the dimension of the eigenspace associated with the eigenvalue  $\lambda_n$  of the Laplace Beltrami operator  $\Delta_d$  (see, e.g., [14]). The equality  $\underset{S(L^2(\mathbb{M}_d, d\nu; \mathbb{C}))}{=}$  means identity in the norm of the space of Hilbert–

Schmidt operators on  $L^2(\mathbb{M}_d, d\nu; \mathbb{C})$ , the space of complex-valued square integrable functions on  $\mathbb{M}_d$ . Specifically, the equality in (2) means that

$$\int_{\mathbb{M}_d \times \mathbb{M}_d} \left| f_\omega(x, y) - \sum_{n=0}^{\infty} f_n(\omega) \sum_{j=1}^{\Gamma(n, d)} S_{n,j}^d(x) S_{n,j}^d(y) \right|^2 d\nu(x) d\nu(y) = 0,$$

where  $f_\omega$  is the kernel of the integral operator  $\mathcal{F}_\omega$ , for every  $\omega \in [-\pi, \pi]$ .

Let  $\{X_t, t = 0, \dots, T-1\}$  be a functional sample of size  $T \geq 2$  of  $X$ . The

fDFT  $\tilde{X}_\omega^{(T)}$  is defined as

$$\tilde{X}_\omega^{(T)}(x) = \frac{1}{\sqrt{2\pi T}} \sum_{t=0}^{T-1} X_t(x) \exp(-i\omega t), \quad x \in \mathbb{M}_d, \quad \omega \in [-\pi, \pi], \quad T \geq 2. \quad (3)$$

The kernel  $p_\omega^{(T)}$  of the periodogram operator  $\mathcal{P}_\omega^{(T)} = \tilde{X}_\omega^{(T)} \otimes \tilde{X}_{-\omega}^{(T)}$  satisfies

$$p_\omega^{(T)}(x, y) = \frac{1}{2\pi T} \sum_{t=0}^{T-1} \sum_{s=0}^{T-1} X_t(x) X_s(y) \exp(-i\omega(t-s)), \quad \forall x, y \in \mathbb{M}_d, \quad (4)$$

for  $\omega \in [-\pi, \pi]$ . We will denote by  $f_\omega^{(T)}(x, y) = \text{cum}(\tilde{X}_\omega^{(T)}(x), \tilde{X}_{-\omega}^{(T)}(y)) = E[p_\omega^{(T)}(x, y)]$ ,  $x, y \in \mathbb{M}_d$ , the kernel of the cumulant operator  $\mathcal{F}_\omega^{(T)}$  of order 2 of the fDFT  $\tilde{X}_\omega^{(T)}$  over the diagonal  $\omega \in [-\pi, \pi]$ . Note that, for  $\omega \in [-\pi, \pi]$ , and  $T \geq 2$ , the Féjer kernel is given by

$$F_T(\omega) = \frac{1}{T} \sum_{t=1}^T \sum_{s=1}^T \exp(-i(t-s)\omega) = \frac{1}{T} \left[ \frac{\sin(T\omega/2)}{\sin(\omega/2)} \right]^2. \quad (5)$$

The weighted periodogram operator denoted as  $\hat{\mathcal{F}}_\omega^{(T)}$  has kernel  $\hat{f}_\omega^{(T)}$  given by, for every  $x, y \in \mathbb{M}_d$ ,

$$\hat{f}_\omega^{(T)}(x, y) = \left[ \frac{2\pi}{T} \right] \sum_{s=1}^{T-1} W^{(T)} \left( \omega - \frac{2\pi s}{T} \right) p_{\frac{2\pi s}{T}}^{(T)}(x, y), \quad \omega \in [-\pi, \pi], \quad (6)$$

where  $W^{(T)}$  is a weight function satisfying

$$W^{(T)}(x) = \sum_{j \in \mathbb{Z}} \frac{1}{B_T} W \left( \frac{x + 2\pi j}{B_T} \right), \quad (7)$$

with  $B_T$  being the positive bandwidth parameter. Function  $W$  is a real-valued function defined on  $\mathbb{R}$  such that  $W$  is positive, even, and bounded in variation;  $W(x) = 0$ , if  $|x| \geq 1$ ;  $\int_{\mathbb{R}} |W(x)|^2 dx < \infty$ ;  $\int_{\mathbb{R}} W(x) dx = 1$ .

## 1.2 Hypothesis testing

The elements involved, and the conditions assumed in the functional spectral domain, characterizing the SRD and LRD scenarios respectively tested under

the null  $H_0$  and the alternative  $H_1$  hypotheses, are now introduced. The proposed test statistics operator based on the weighted periodogram operator is also formulated.

Stationary SRD functional time series are characterized by the summability of the series of trace norms of the elements of the family of covariance operators  $\{\mathcal{R}_\tau, \tau \in \mathbb{Z}\}$  (see, e.g., [20]). That is,  $X$  displays SRD if and only if  $\sum_{\tau \in \mathbb{Z}} \|\mathcal{R}_\tau\|_{L^1(L^2(\mathbb{M}_d, d\nu, \mathbb{R}))} < \infty$ , where  $L^1(L^2(\mathbb{M}_d, d\nu, \mathbb{R}))$  denotes the space of trace operators on  $L^2(\mathbb{M}_d, d\nu, \mathbb{R})$ . In our setting this condition can be formulated as follows:

$$\sum_{\tau \in \mathbb{Z}} \|\mathcal{R}_\tau\|_{L^1(L^2(\mathbb{M}_d, d\nu, \mathbb{R}))} = \sum_{\tau \in \mathbb{Z}} \sum_{n \in \mathbb{N}_0} \Gamma(n, d) \left| \int_{-\pi}^{\pi} \exp(i\omega\tau) f_n(\omega) d\omega \right| < \infty. \quad (8)$$

When (8) fails,  $X$  is said to display LRD. In the following, we will adopt the LRD scenario introduced in [28], given by

$$\mathcal{F}_\omega = \mathcal{M}_\omega |\omega|^{-\mathcal{A}}, \quad \omega \in [-\pi, \pi], \quad (9)$$

where the invariant positive self-adjoint operators  $\mathcal{M}_\omega$  and  $|\omega|^{-\mathcal{A}}$  are composed. Specifically,  $\mathcal{A}$  denotes the LRD operator on  $L^2(\mathbb{M}_d, d\nu; \mathbb{C})$ . Operator  $|\omega|^{-\mathcal{A}}$  in (9) is interpreted as in [23] and [24], where  $\mathcal{A}$  plays the role of operator-valued Hurst coefficient in the setting of fractional Brownian motion introduced in this framework. Moreover, operator  $\mathcal{M}_\omega$  is the regular spectral operator reflecting markovianess when the null space of  $\mathcal{A}$  coincides with  $L^2(\mathbb{M}_d, d\nu; \mathbb{C})$ . Thus,

$$\sum_{\tau \in \mathbb{Z}} \left\| \int_{[-\pi, \pi]} \exp(i\omega\tau) \mathcal{M}_\omega d\omega \right\|_{L^1(L^2(\mathbb{M}_d, d\nu, \mathbb{R}))} < \infty, \quad (10)$$

where, here, and through the paper, the operator integrals are understood as improper operator Stieltjes integrals which converge strongly (see, e.g., Section 8.2.1 in [25]).

We will apply the spectral theory of self-adjoint operators (see, e.g., [7]) in terms of the common spectral kernel

$$\Upsilon(x, y) = \sum_{n \in \mathbb{N}_0} \sum_{j=1}^{\Gamma(n, d)} S_{n,j}^d(x) \overline{S_{n,j}^d(y)}, \quad x, y \in \mathbb{M}_d,$$

under the assumed invariance property with respect to the group of isometries of  $\mathbb{M}_d$ .

The point spectrum of  $\mathcal{A}$  is given by  $\{\alpha(n), n \in \mathbb{N}_0\}$ , with  $l_\alpha \leq \alpha(n) \leq L_\alpha$ , for every  $n \in \mathbb{N}_0$ , and  $l_\alpha, L_\alpha \in (0, 1/2)$ . It is assumed that LRD operator  $\mathcal{A}$  has

kernel  $\mathcal{K}_{\mathcal{A}}$  admitting the following series expansion in the weak-sense:

$$\mathcal{K}_{\mathcal{A}}(x, y) = \sum_{n \in \mathbb{N}_0} \alpha(n) \sum_{j=1}^{\Gamma(n,d)} S_{n,j}^d \otimes \overline{S_{n,j}^d}(x, y), \quad x, y \in \mathbb{M}_d. \quad (11)$$

Specifically, identity (11) is understood in the following sense, for every  $f, g \in C^\infty(\mathbb{M}_d)$ , the space of infinitely differentiable functions with compact support in  $\mathbb{M}_d$ ,

$$\mathcal{A}(f)(g) = \int_{\mathbb{M}_d \times \mathbb{M}_d} f(x)g(y) \sum_{n \in \mathbb{N}_0} \alpha(n) \sum_{j=1}^{\Gamma(n,d)} S_{n,j}^d(x) \overline{S_{n,j}^d}(y) d\nu(x) d\nu(y). \quad (12)$$

Note that, under the conditions assumed,  $\mathcal{A}$  and  $\mathcal{A}^{-1}$  are bounded, and  $\|\mathcal{A}\|_{\mathcal{L}(L^2(\mathbb{M}_d, d\nu, \mathbb{R}))} < 1/2$ , with  $\|\cdot\|_{\mathcal{L}(L^2(\mathbb{M}_d, d\nu, \mathbb{R}))}$  denoting the norm in the space  $\mathcal{L}(L^2(\mathbb{M}_d, d\nu, \mathbb{R}))$  of bounded linear operators on  $L^2(\mathbb{M}_d, d\nu, \mathbb{R})$ .

In a similar way, operator  $|\omega|^{-\mathcal{A}}$  is interpreted as

$$|\omega|^{-\mathcal{A}}(f)(g) = \int_{\mathbb{M}_d \times \mathbb{M}_d} f(x)g(y) \sum_{n \in \mathbb{N}_0} \frac{1}{|\omega|^{\alpha(n)}} \sum_{j=1}^{\Gamma(n,d)} S_{n,j}^d \otimes \overline{S_{n,j}^d}(x, y), d\nu(x) d\nu(y), \quad (13)$$

for every  $f, g \in C^\infty(\mathbb{M}_d)$  and  $\omega \in [-\pi, \pi] \setminus \{0\}$ .

For every  $\omega \in [-\pi, \pi]$ , operator  $\mathcal{M}_\omega$  in (9) is a Hilbert-Schmidt operator on  $L^2(\mathbb{M}_d, d\nu; \mathbb{C})$ , whose kernel  $\mathcal{K}_{\mathcal{M}_\omega}(x, y)$  admits the following series expansion in the norm of the space  $\mathcal{S}(L^2(\mathbb{M}_d, d\nu; \mathbb{C}))$ :

$$\mathcal{K}_{\mathcal{M}_\omega}(x, y) = \sum_{n \in \mathbb{N}_0} M_n(\omega) \sum_{j=1}^{\Gamma(n,d)} S_{n,j}^d \otimes \overline{S_{n,j}^d}(x, y), \quad x, y \in \mathbb{M}_d, \quad (14)$$

where  $\{M_n(\omega), n \in \mathbb{N}_0\}$  denotes the sequence of positive eigenvalues. For each  $n \in \mathbb{N}_0$ ,  $M_n(\omega), \omega \in [-\pi, \pi]$ , is a continuous positive slowly varying function at  $\omega = 0$  in the Zygmund's sense (see Definition 6.6 in [1], and **Assumption IV** in [28]). Equation (10) can be rewritten, in terms of  $\{M_n(\omega), n \in \mathbb{N}_0, \omega \in [-\pi, \pi]\}$ , as follows:

$$\sum_{\tau \in \mathbb{Z}} \sum_{n \in \mathbb{N}_0} \Gamma(n, d) \left| \int_{-\pi}^{\pi} \exp(i\omega\tau) M_n(\omega) d\omega \right| < \infty. \quad (15)$$

Equation (15) implies that  $X$  displays SRD, when  $\alpha(n) = 0$ , for every  $n \in \mathbb{N}_0$ . Under (15),  $\{\mathcal{M}_\omega, \omega \in [-\pi, \pi]\}$  is also included in the trace class.

Under the above setting of conditions,

$$\int_{-\pi}^{\pi} \|\mathcal{F}_\omega\|_{\mathcal{S}(L^2(\mathbb{M}_d, d\nu, \mathbb{C}))}^2 d\omega < \infty, \quad (16)$$



i.e.,  $\|\mathcal{F}_\omega\|_{\mathcal{S}(L^2(\mathbb{M}_d, d\nu, \mathbb{C}))} \in L^2([-\pi, \pi])$ , with  $L^2([-\pi, \pi])$  being the space of square integrable functions on the interval  $[-\pi, \pi]$ . Condition (16) plays a crucial role in the derivation of the results of this paper under LRD.

From equations (9)–(14), the positive frequency varying eigenvalue sequence  $\{f_n(\omega), n \in \mathbb{N}_0\}$  in (2) admits the following expression:

$$f_n(\omega) = \frac{M_n(\omega)}{|\omega|^{\alpha(n)}}, \quad \omega \in [-\pi, \pi], \quad n \in \mathbb{N}_0. \quad (17)$$

Note that, since  $\sin(\omega) \sim \omega, \omega \rightarrow 0$ ,

$$|1 - \exp(-i\omega)|^{-A} = [4 \sin^2(\omega/2)]^{-A/2} \sim |\omega|^{-A}, \quad \omega \rightarrow 0. \quad (18)$$

Sequence (17) is involved in our proposal for testing SRD against LRD in the spectral domain, in the context of  $\mathbb{M}_d$ -supported functional time series. Specifically, the following testing problem is considered:

$$H_0 : f_n(\omega) = M_n(\omega), \quad \omega \in [-\pi, \pi], \quad \forall n \in \mathbb{N}_0 \quad (19)$$

$$H_1 : f_n(\omega) = M_n(\omega) |\omega|^{-\alpha(n)}, \quad \omega \in [-\pi, \pi], \quad \forall n \in \mathbb{N}_0. \quad (20)$$

Our main goal is to designing a consistent test operator statistics in the spectral domain. Such a design must capture the singularities at zero frequency at different manifold resolution levels when  $H_1$  in (20) holds. To this aim, our test operator statistics, denoted as  $\mathcal{S}_{B_T}$ , is defined under the integral sign as the product of a scaled weighted periodogram operator, and a truncated Dirac Delta distribution depending on the functional sample size. This integral formulation approximates in a suitable way the functional spectral behavior at zero frequency. Specifically,

$$\mathcal{S}_{B_T} = \sqrt{B_T T} \int_{[-\sqrt{B_T}/2, \sqrt{B_T}/2]} \widehat{\mathcal{F}}_\omega^{(T)} \frac{d\omega}{\sqrt{B_T}}, \quad (21)$$

where the kernel of the integral operator  $\widehat{\mathcal{F}}_\omega^{(T)}$  has been introduced in equation (6), with, as before,  $B_T$  being the bandwidth parameter. Denote by  $\mathbb{I}_{[-\sqrt{B_T}/2, \sqrt{B_T}/2]}$  the indicator function on the interval  $[-\sqrt{B_T}/2, \sqrt{B_T}/2]$ . Note that  $\frac{\mathbb{I}_{[-\sqrt{B_T}/2, \sqrt{B_T}/2]}}{\sqrt{B_T}}$  converges in the weak sense, i.e., in the sense of generalized functions (see [10]), to a Dirac Delta distribution at frequency zero, as  $T \rightarrow \infty$ .

## 2 Preliminary results under SRD

The following lemmas will be applied in the proof of Theorem 1 on the asymptotic normality of  $\mathcal{S}_{B_T}$  under  $H_0$ . Specifically, Lemmas 1–3 provide the asymptotic

unbiasedness of the weighted periodogram operator in the space  $L^2(\mathbb{M}_d^2, d\nu \otimes d\nu, \mathbb{C})$ , and its consistency and asymptotic Gaussian distribution under  $H_0$ . Their proofs can be obtained in the same way as in [20], where these results are established for the separable Hilbert space  $H = L^2([0, 1], \mathbb{C})$ . The orthogonal expansion provided in Lemma 4 constitutes a key technical tool in the derivation of the proof of Theorem 1.

**Lemma 1** *Assume that*

$$\sum_{t \in \mathbb{Z}} (1 + |t|) \|cum(X_t, X_0)\|_{L^2(\mathbb{M}_d^2, d\nu \otimes d\nu, \mathbb{R})} < \infty,$$

and that  $B_T \rightarrow 0$  and  $B_T T \rightarrow \infty$  as  $T \rightarrow \infty$ . Then, for every  $x, y \in \mathbb{M}_d$ ,

$$E[\widehat{f}_\omega^{(T)}(x, y)] = \int_{\mathbb{R}} W(\xi) f_{\omega - \xi B_T}(x, y) d\xi + \mathcal{O}(B_T^{-1} T^{-1}), \quad T \rightarrow \infty, \quad (22)$$

where equality holds in  $L^2(\mathbb{M}_d^2, d\nu \otimes d\nu, \mathbb{C})$ , and the asymptotic order of the error term holds uniformly in  $\omega$ .

**Proof.** See Proposition 3.1 in [20].

Suitable summability conditions in time of the norm in  $L^2(\mathbb{M}_d^4, \otimes_{i=1}^4 d\nu(x_i), \mathbb{R})$  of the fourth-order cumulant operators ensure the consistency of the weighted periodogram operator in Lemma 2.

**Lemma 2** *Assume that, as before,  $B_T \rightarrow 0$  and  $B_T T \rightarrow \infty$  as  $T \rightarrow \infty$ , and*

$$\begin{aligned} \sum_{t \in \mathbb{Z}} (1 + |t|) \|cum(X_t, X_0)\|_{L^2(\mathbb{M}_d^2, d\nu \otimes d\nu, \mathbb{R})} < \infty, \\ \sum_{t_1, t_2, t_3 \in \mathbb{Z}} (1 + |t_j|) \|cum(X_{t_1}, X_{t_2}, X_{t_3}, X_0)\|_{L^2(\mathbb{M}_d^4, \otimes_{i=1}^4 d\nu(x_i), \mathbb{R})} < \infty, \quad j = 1, 2, 3, \end{aligned} \quad (23)$$

holds. Then, as  $T \rightarrow \infty$ , the integrated mean square error (IMSE) satisfies

$$\begin{aligned} IMSE(\mathcal{F}^{(T)}) &= \int_{-\pi}^{\pi} E \|\widehat{\mathcal{F}}_\omega^{(T)} - \mathcal{F}_\omega\|_{\mathcal{S}(L^2(\mathbb{M}_d^2, d\nu \otimes d\nu, \mathbb{C}))} d\omega \\ &= \mathcal{O}(B_T^2) + \mathcal{O}(B_T^{-1} T^{-1}), \end{aligned} \quad (24)$$

and

$$\begin{aligned} E \left[ \|\widehat{\mathcal{F}}_\omega^{(T)} - \mathcal{F}_\omega\|_{\mathcal{S}(L^2(\mathbb{M}_d^2, d\nu \otimes d\nu, \mathbb{C}))} \right] &= \mathcal{O}(B_T^2) + \mathcal{O}(B_T^{-1} T^{-1}), \quad \omega \in (-\pi, \pi), \\ E \left[ \|\widehat{\mathcal{F}}_\omega^{(T)} - \mathcal{F}_\omega\|_{\mathcal{S}(L^2(\mathbb{M}_d^2, d\nu \otimes d\nu, \mathbb{C}))} \right] &= \mathcal{O}(B_T^2) + \mathcal{O}(B_T^{-2} T^{-1}), \quad \omega = 0, \pm\pi. \end{aligned}$$

**Proof.** See Theorem 3.6 in [20].

Lemma 3 provides the asymptotic infinite-dimensional Gaussian distribution of the weighted periodogram operator

**Lemma 3** *Assume that  $E\|X_0\|^k < \infty$ , for all  $k \geq 2$ , and*

$$(i) \sum_{t_1, \dots, t_{k-1} \in \mathbb{Z}} \|\text{cum}(X_{t_1}, \dots, X_{t_{k-1}}, X_0)\|_{L^2(\mathbb{M}_d^k, \otimes_{i=1}^k d\nu(x_i), \mathbb{R})} < \infty$$

$$(i') \sum_{t_1, \dots, t_{k-1} \in \mathbb{Z}} (1 + |t_j|) \|\text{cum}(X_{t_1}, \dots, X_{t_{k-1}}, X_0)\|_{L^2(\mathbb{M}_d^k, \otimes_{i=1}^k d\nu(x_i), \mathbb{R})} < \infty, \\ \text{for } k \in \{2, 4\}, j < k$$

$$(ii) \sum_{t \in \mathbb{Z}} (1 + |t|) \|\mathcal{R}_t\|_{L^1(L^2(\mathbb{M}_d, d\nu, \mathbb{R}))} < \infty$$

$$(iii) \sum_{t_1, t_2, t_3 \in \mathbb{Z}} \|\mathcal{R}_{t_1, t_2, t_3}\|_{L^1(L^2(\mathbb{M}_d^2, \otimes_{i=1}^2 d\nu(x_i), \mathbb{R}))} < \infty.$$

Then, for every frequencies  $\omega_j$ ,  $j = 1, \dots, J$ , with  $J < \infty$ ,

$$\sqrt{B_T} T(\widehat{f}_{\omega_j}^{(T)} - E[\widehat{f}_{\omega_j}^{(T)}]) \rightarrow_D \widehat{f}_{\omega_j}, \quad j = 1, \dots, J \quad (25)$$

where  $\rightarrow_D$  denotes the convergence in distribution. Here,  $\widehat{f}_{\omega_j}$ ,  $j = 1, \dots, J$ , are zero-mean complex Gaussian elements in  $\mathcal{S}(L^2(\mathbb{M}_d, d\nu, \mathbb{C})) = L^2(\mathbb{M}_d^2, d\nu \otimes d\nu, \mathbb{C})$ , with covariance kernel:

$$\text{cov}(\widehat{f}_{\omega_i}(x_1, y_1), \widehat{f}_{\omega_j}(x_2, y_2)) = \|W\|_{L^2(\mathbb{R})}^2 \{ \eta(\omega_i - \omega_j) f_{\omega_i}(x_1, x_2) f_{-\omega_i}(y_1, y_2) \\ + \eta(\omega_i + \omega_j) f_{\omega_i}(x_1, y_2) f_{-\omega_i}(y_1, x_2) \}, \quad (x_i, y_i) \in \mathbb{M}_d^2, \quad i = 1, 2, \quad (26)$$

with  $\eta(\omega) = 1$ , for  $\omega \in 2\pi\mathbb{Z}$ , and  $\eta(\omega) = 0$ , otherwise. Thus,  $\widehat{f}_{\omega_i}$  and  $\widehat{f}_{\omega_j}$  are independent for  $\omega_i + \omega_j \neq 0, \text{ mod } 2\pi$  and  $\omega_i - \omega_j \neq 0, \text{ mod } 2\pi$ . For zero frequency modulus  $2\pi$  the limit Gaussian random element is in  $\mathcal{S}(L^2(\mathbb{M}_d, d\nu, \mathbb{R})) = L^2(\mathbb{M}_d^2, d\nu \otimes d\nu, \mathbb{R})$ .

**Proof.** See Theorem 3.7 in [20].

As commented, the next lemma will be applied in the derivation of Theorem 1 below. It provides the Karhunen–Loève expansion of the limit Gaussian random element obtained in Lemma 3, in terms of the following random Fourier coefficients: For each  $\omega \in [-\pi, \pi]$ ,

$$Y_{n,j,h,l}^{(\infty)}(\omega) = \frac{(\|W\|_{L^2(\mathbb{R})})^{-1}}{\sqrt{f_n(\omega)f_h(\omega)}} \int_{\mathbb{M}_d^2} \widehat{f}_\omega(\tau, \sigma) S_{n,j}^d(\tau) \overline{S_{h,l}^d(\sigma)} d\nu(\sigma) d\nu(\tau) \\ \widetilde{Y}_{n,j,h,l}^{(\infty)}(\omega) = \frac{(\|W\|_{L^2(\mathbb{R})})^{-1}}{\sqrt{f_n(\omega)f_h(\omega)}} \int_{\mathbb{M}_d^2} \widehat{f}_\omega(\tau, \sigma) \overline{S_{h,l}^d(\tau)} S_{n,j}^d(\sigma) d\nu(\sigma) d\nu(\tau) \\ = \overline{Y_{h,l,n,j}^{(\infty)}(\omega)}, \quad j = 1, \dots, \Gamma(n, d), \quad l = 1, \dots, \Gamma(h, d), \quad n, h \in \mathbb{N}_0, \quad (27)$$

where integration is understood in the mean-square sense.

**Lemma 4** *Let  $\widehat{f}_\omega$  be the kernel of the limit Gaussian random element, in the space  $\mathcal{S}(L^2(\mathbb{M}_d, d\nu, \mathbb{C}))$ , introduced in Lemma 3. Then, the following series expansion holds in the mean-square sense: For every  $(\tau, \sigma) \in \mathbb{M}_d^2$ ,*

$$\begin{aligned} \frac{1}{\|W\|_{L^2(\mathbb{R})}} \widehat{f}_\omega(\tau, \sigma) &= \sum_{n,h \in \mathbb{N}_0} \sum_{j=1}^{\Gamma(n,d)} \sum_{l=1}^{\Gamma(h,d)} \sqrt{f_n(\omega) f_h(\omega)} \\ &\times [Y_{n,j,h,l}^{(\infty)}(\omega) + \mathbb{I}_{\{0,\pi\}} \widetilde{Y}_{n,j,h,l}^{(\infty)}(\omega)] S_{n,j}^d(\tau) \overline{S_{h,l}^d(\sigma)}, \end{aligned} \quad (28)$$

where  $\mathbb{I}_{\{0,\pi\}}$  denotes the indicator function of the set  $\{0,\pi\}$ . Here,  $\mathcal{L}_{\mathcal{S}(L^2(\mathbb{M}_d, d\nu; \mathbb{C}))}(\Omega, \mathcal{A}, \mathcal{P})$  denotes the space of zero-mean second-order  $\mathcal{S}(L^2(\mathbb{M}_d, d\nu; \mathbb{C}))$ -valued random variables with the norm  $\sqrt{E\|\cdot\|_{\mathcal{S}(L^2(\mathbb{M}_d, d\nu; \mathbb{C}))}^2}$ .

The random Fourier coefficients  $\{Y_{n,j,h,l}^{(\infty)}(\omega)\}$  and  $\{\widetilde{Y}_{n,j,h,l}^{(\infty)}(\omega)\}$  have been introduced in equation (27). They are independent and identically distributed standard complex-valued Gaussian random variables.

**Proof.** See Section A.1 of Appendices.

The next result derives the asymptotic Gaussian distribution of the test statistics operator  $\mathcal{S}_{B_T}$  in (21), involving its suitable centering under  $H_0$ . As given in the proof of this result (see Section A.2 of the Appendices), the convergence to a Gaussian random element in the norm of the space  $\mathcal{L}_{\mathcal{S}(L^2(\mathbb{M}_d, d\nu, \mathbb{C}))}^2(\Omega, \mathcal{A}, P)$  also holds.

**Theorem 1** *Under  $H_0$ , assume that the conditions in Lemma 3 hold. Then,*

$$\mathcal{S}_{B_T} - E[\mathcal{S}_{B_T}] \rightarrow_D Y_0^{(\infty)}, \quad T \rightarrow \infty, \quad (29)$$

where  $\mathcal{S}_{B_T}$  has been introduced in (21), and  $Y_0^{(\infty)}$  is a zero-mean Gaussian random element in  $\mathcal{S}(L^2(\mathbb{M}_d, d\nu, \mathbb{R}))$ , whose autocovariance operator  $\mathcal{R}_{Y_0^{(\infty)}} = E[Y_0^{(\infty)} \otimes Y_0^{(\infty)}]$  has kernel defined from equation (26) in Lemma 3, considering  $\omega_i = \omega_j = 0$ .

**Proof.** See Section A.2 of the Appendices.

### 3 Bias second and fourth order asymptotics under LRD

New results on the bias asymptotics of the integrated second and fourth order empirical cumulant spectral density operators of  $X$  under  $H_1$  are obtained in

this section. They allow to state similar properties, for the integrated weighted periodogram operator under LRD, to those ones established in previous Lemmas 1 and 2 (see also Theorem 2 and Corollary 2 in Section 4).

The rate of convergence to zero of the bias of the integrated periodogram operator in the space  $\mathcal{S}(L^2(\mathbb{M}_d, d\nu, \mathbb{C}))$  is obtained here under LRD. The proof of this result (see Section B.1 of the Appendices) exploits (16) in a similar way to Theorem 1 in [28], and the tools available in our particular setting, leading to some differences with respect to Theorem 1 in [28], where a more general setting is considered. The following well-known identity will be applied through the proof of this result:

$$\mathcal{F}_\omega^{(T)} = E [p_\omega^{(T)}] = [F_T * \mathcal{F}_\bullet](\omega) = \int_{-\pi}^{\pi} F_T(\omega - \xi) \mathcal{F}_\xi d\xi, \quad T \geq 2, \quad (30)$$

for every  $\omega \in [-\pi, \pi] \setminus \{0\}$ , where  $F_T(\omega)$  denotes the Féjer kernel in (5) of Section 1.1.

**Lemma 5** *Under  $H_1$ ,*

$$\int_{-\pi}^{\pi} \mathcal{F}_\omega^{(T)} d\omega = \int_{-\pi}^{\pi} \mathcal{F}_\omega d\omega + \mathcal{O}(T^{-1}), \quad T \rightarrow \infty, \quad (31)$$

*in the norm of  $\mathcal{S}(L^2(\mathbb{M}_d, d\nu, \mathbb{C}))$ .*

**Proof.** See Section B.1 of the Appendices.

The following corollary is obtained from Lemma 5, and provides the convergence to zero of the bias of the integrated weighted periodogram operator under  $H_1$ .

**Corollary 1** *Under  $H_1$ , as  $T \rightarrow \infty$ ,*

$$\int_{-\pi}^{\pi} E_{H_1}[\widehat{\mathcal{F}}_\omega^{(T)}] d\omega \underset{\mathcal{S}(L^2(\mathbb{M}_d, d\nu, \mathbb{C}))}{=} \int_{-\pi}^{\pi} \int_{\mathbb{R}} W(\xi) \mathcal{F}_{\omega - \xi B_T} d\xi d\omega + \mathcal{O}(B_T^{-1} T^{-1}) + \mathcal{O}(T^{-1}), \quad (32)$$

*where  $E_{H_1}$  denotes expectation under the alternative  $H_1$ .*

**Proof.** See Section B.2 of the Appendices.

The rate of convergence to zero, in the space  $\mathcal{S}(L^2(\mathbb{M}_d^2, \otimes_{i=1}^2 \nu(dx_i), \mathbb{C})) \equiv L^2(\mathbb{M}_d^4, \otimes_{i=1}^4 \nu(dx_i), \mathbb{C})$ , of the bias of the integrated fourth-order empirical cumulant spectral density operators of  $X$  under LRD is obtained in Lemma 6 below. The following assumption is required:

Assumption A1. The following convergence holds:

$$\sum_{t_1, t_2, t_3 \in \mathbb{Z}} \|\text{cum}(X_{t_1}, X_{t_2}, X_{t_3}, X_0)\|_{L^2(\mathbb{M}_d^4, \otimes_{i=1}^4 d\nu(x_i), \mathbb{R})}^2 < \infty, \quad (33)$$

where

$$\begin{aligned} & \|\text{cum}(X_{t_1}, X_{t_2}, X_{t_3}, X_0)\|_{L^2(\mathbb{M}_d^4, \otimes_{i=1}^4 d\nu(dx_i), \mathbb{R})}^2 \\ &= \int_{\mathbb{M}_d^4} |\text{cum}(X_{t_1}(x), X_{t_2}(y), X_{t_3}(z), X_0(v))|^2 d\nu(x) d\nu(y) d\nu(z) d\nu(v). \end{aligned}$$

**Lemma 6** Under  $H_1$  and Assumption A1, uniformly in  $\omega_4 \in [-\pi, \pi]$ ,

$$\begin{aligned} & \int_{[-\pi, \pi]^3} T \text{cum}\left(\tilde{X}_{\omega_1}^{(T)}(\tau_1), \tilde{X}_{\omega_2}^{(T)}(\tau_2), \tilde{X}_{\omega_3}^{(T)}(\tau_3), \tilde{X}_{\omega_4}^{(T)}(\tau_4)\right) d\omega_1 d\omega_2 d\omega_3 \\ & \stackrel{=}{=} \mathcal{S}(L^2(\mathbb{M}_d^2, \otimes_{i=1}^2 \nu(dx_i), \mathbb{C})) \int_{[-\pi, \pi]^3} \mathcal{F}_{\omega_1, \omega_2, \omega_3}(\tau_1, \tau_2, \tau_3, \tau_4) d\omega_1 d\omega_2 d\omega_3 + \mathcal{O}(T^{-1}), \end{aligned} \quad (34)$$

where, for  $\omega_i \in [-\pi, \pi]$ ,  $i = 1, 2, 3$ ,

$$\mathcal{F}_{\omega_1, \omega_2, \omega_3} \stackrel{=}{=} \mathcal{S}(L^2(\mathbb{M}_d^2, \otimes_{i=1}^2 \nu(dx_i), \mathbb{C})) \frac{1}{(2\pi)^3} \sum_{t_1, t_2, t_3 = -\infty}^{\infty} \exp\left(\sum_{j=1}^3 \omega_j t_j\right) \text{cum}(X_{t_1}, X_{t_2}, X_{t_3}, X_0) \quad (35)$$

denotes the cumulant spectral density operator of order 4 of  $X$ , and, as before,  $\mathcal{S}(L^2(\mathbb{M}_d^2, \otimes_{i=1}^2 \nu(dx_i), \mathbb{C})) \stackrel{=}{=} L^2(\mathbb{M}_d^4, \otimes_{i=1}^4 d\nu(x_i), \mathbb{C})$ .

**Proof.** See Section B.3 of the Appendices. .

## 4 A test for LRD in $\mathbb{M}_d$ -supported functional time series

Consistency of the test based on  $\mathcal{S}_{B_T}$  is derived in this section. Specifically, Theorem 3 provides the almost surely divergence in the norm of the space

$\mathcal{S}(L^2(\mathbb{M}_d, d\nu, \mathbb{C}))$  of  $\mathcal{S}_{B_T}$  under  $H_1$ . The proof of this result follows, from Proposition 1 showing the divergence in the norm of the space  $\mathcal{S}(L^2(\mathbb{M}_d, d\nu, \mathbb{C}))$  of the centering operator of  $\mathcal{S}_{B_T}$ , and from Theorem 2 and Corollary 2, establishing the consistency of the integrated weighted periodogram operator under  $H_1$ . The implementation of the testing procedure in practice is also discussed.

**Proposition 1** *Under  $H_1$ , as  $T \rightarrow \infty$ ,*

$$\left\| \int_{[-\sqrt{B_T}/2, \sqrt{B_T}/2]} E_{H_1}[\widehat{\mathcal{F}}_\omega^{(T)}] \frac{d\omega}{\sqrt{B_T}} \right\|_{\mathcal{S}(L^2(\mathbb{M}_d, d\nu, \mathbb{C}))} \geq g(T) = \mathcal{O}(B_T^{-l_\alpha - 1/2}). \quad (36)$$

**Proof.** See Section C.1 of the Appendices.

**Theorem 2** *Assume that Assumptions A1 holds, and that*

$$\int_{[-\pi, \pi]} \|\mathcal{M}_\omega\|_{L^1(L^2(\mathbb{M}_d, d\nu, \mathbb{C}))}^2 |\omega|^{-2L_\alpha} d\omega < \infty. \quad (37)$$

*Then, under  $H_1$ , as  $T \rightarrow \infty$ ,*

$$\int_{-\pi}^{\pi} E_{H_1} \left\| \widehat{\mathcal{F}}_\omega^{(T)} - E_{H_1}[\widehat{\mathcal{F}}_\omega^{(T)}] \right\|_{\mathcal{S}(L^2(\mathbb{M}_d, d\nu, \mathbb{C}))}^2 d\omega \leq h(T) = \mathcal{O}(B_T^{-1} T^{-1}). \quad (38)$$

**Proof.** See Section C.2 of the Appendices.

From Theorem 2, consistency in mean under  $H_1$ , in the norm of  $\mathcal{S}(L^2(\mathbb{M}_d, d\nu, \mathbb{C}))$ , of the integrated weighted periodogram operator follows.

**Corollary 2** *Under the conditions of Theorem 2, as  $T \rightarrow \infty$ ,*

$$\left\| \int_{-\pi}^{\pi} E_{H_1} \left[ \widehat{\mathcal{F}}_\omega^{(T)} - \int_{-\pi}^{\pi} W(\xi) \mathcal{F}_{\omega - B_T \xi} d\xi \right] d\omega \right\|_{\mathcal{S}(L^2(\mathbb{M}_d, d\nu, \mathbb{C}))} \leq \tilde{g}(T) = \mathcal{O}(T^{-1/2} B_T^{-1/2}).$$

**Proof.** See Section C.3 of the Appendices.

Under the conditions assumed in the following result,  $\mathcal{S}_{B_T}$  in (21) allows to testing (19)–(20) in a consistent way.

**Theorem 3** *Under  $H_1$ , assume that  $l_\alpha > 1/4$ , and that the bandwidth parameter  $B_T = T^{-\beta}$  for  $\beta \in (0, 1)$ . If conditions of Theorem 2 hold, then, as  $T \rightarrow \infty$ ,*

$$\|\mathcal{S}_{B_T}\|_{\mathcal{S}(L^2(\mathbb{M}_d, d\nu, \mathbb{C}))} \rightarrow a.s. \infty,$$

*where  $\rightarrow_{a.s.} \infty$  denotes almost surely divergence.*

**Proof.** See Section C.4 of the Appendices.

Theorem 3 motivates the methodology to be adopted in practice. Specifically, as illustrated in the simulation study undertaken in the next section, a consistent test for long memory is obtained by rejecting  $H_0$ , when, for every  $j = 1, \dots, \Gamma(n, d)$ ,  $l = 1, \dots, \Gamma(h, d)$ ,  $n, h \in \mathbb{N}_0$ ,

$$\frac{|[S_{B_T} - E[S_{B_T}]](S_{h,l}^d)(S_{n,j}^d)|}{\sqrt{\text{Var}(S_{B_T}(S_{h,l}^d)(S_{n,j}^d))}} \quad (39)$$

is larger than an upper tail standard normal critical value, according to Lemma 4 and Theorem 1. Here, for  $j = 1, \dots, \Gamma(n, d)$ ,  $l = 1, \dots, \Gamma(h, d)$ ,  $n, h \in \mathbb{N}_0$ ,

$$\begin{aligned} [S_{B_T} - E[S_{B_T}]](S_{h,l}^d)(S_{n,j}^d) &= \int_{\mathbb{M}_d^2} [S_{B_T} - E[S_{B_T}]](\tau, \sigma) \\ &\quad \times \overline{S_{n,j}^d}(\tau) S_{h,l}^d(\sigma) d\nu(\sigma) d\nu(\tau) \\ \text{Var}(S_{B_T}(S_{h,l}^d)(S_{n,j}^d)) &= \text{Var}\left(\int_{\mathbb{M}_d^2} S_{B_T}(\tau, \sigma) \overline{S_{n,j}^d}(\tau) S_{h,l}^d(\sigma) d\nu(\sigma) d\nu(\tau)\right) \\ &= \frac{2\pi T B_T}{T} \int_{[-\sqrt{B_T}/2, \sqrt{B_T}/2]} \left| \int_{-\pi}^{\pi} W^{(T)}(\omega - \alpha) W^{(T)}(\omega - \alpha) f_n(\alpha) f_h(\alpha) d\alpha \right| \frac{d\omega}{\sqrt{B_T}} \\ &\quad + \frac{2\pi T B_T}{T} \int_{[-\sqrt{B_T}/2, \sqrt{B_T}/2]} \left| \int_{-\pi}^{\pi} W^{(T)}(\omega - \alpha) W^{(T)}(\omega + \alpha) f_n(\alpha) f_h(\alpha) d\alpha \right| \frac{d\omega}{\sqrt{B_T}} \\ &\quad + \mathcal{O}(B_T^{-2} T^{-2}) + \mathcal{O}(T^{-1}) \\ &= \int_{[-\sqrt{B_T}/2, \sqrt{B_T}/2]} \left| \int_{-\pi}^{\pi} \frac{2\pi}{\sqrt{B_T}} W\left(\frac{\omega - \alpha}{B_T}\right) \frac{1}{\sqrt{B_T}} W\left(\frac{\omega - \alpha}{B_T}\right) f_n(\alpha) f_h(\alpha) d\alpha \right| \frac{d\omega}{\sqrt{B_T}} \\ &\quad + \int_{[-\sqrt{B_T}/2, \sqrt{B_T}/2]} \left| \int_{-\pi}^{\pi} \frac{2\pi}{\sqrt{B_T}} W\left(\frac{\omega - \alpha}{B_T}\right) \frac{1}{\sqrt{B_T}} W\left(\frac{\omega + \alpha}{B_T}\right) f_n(\alpha) f_h(\alpha) d\alpha \right| \frac{d\omega}{\sqrt{B_T}} \\ &\quad + \mathcal{O}(B_T^{-2} T^{-2}) + \mathcal{O}(T^{-1}). \end{aligned}$$

The dimensionality problem associated with the above described testing procedure can be substantially alleviate if we restrict our attention to the case where all moments of  $S_{B_T}$  are finite and satisfy the Carleman condition. In that case, one can apply Theorem 4.1 in [5], allowing the testing procedure to be implemented, conditionally to the functional value  $\mathbf{k}$  generated from an  $\mathcal{S}(L^2(\mathbb{M}_d, d\nu; \mathbb{C}))$ -valued Gaussian random variable, with probability measure  $\mu$  on  $\mathcal{S}(L^2(\mathbb{M}_d, d\nu; \mathbb{C}))$ . Specifically,  $H_0$  is tested in terms of  $H_0^{\mathbf{k}}$  defined from the



random projected statistics

$$\mathcal{T}_{B_T}^{\mathbf{k}} = \frac{\left| \langle S_{B_T} - E[S_{B_T}], \mathbf{k} \rangle_{\mathcal{S}(L^2(\mathbb{M}_d, d\nu; \mathbb{C}))} \right|}{\sqrt{\text{Var} \left( \langle S_{B_T} - E[S_{B_T}], \mathbf{k} \rangle_{\mathcal{S}(L^2(\mathbb{M}_d, d\nu; \mathbb{C}))} \right)}}. \quad (40)$$

According to Theorem 4.1 in [5], if  $H_0$  holds, then  $H_0^{\mathbf{k}}$  also holds, and if  $H_0$  fails then  $H_0^{\mathbf{k}}$  also fails  $\mu$ -a.s. Thus, with probability one, we will generate a realization of random direction  $\mathbf{k}$  in  $\mathcal{S}(L^2(\mathbb{M}_d, d\nu; \mathbb{C}))$  for which  $H_0^{\mathbf{k}}$  fails. As before,  $H_0^{\mathbf{k}}$  will be rejected if the observed value of  $\mathcal{T}_{B_T}^{\mathbf{k}}$  is larger than an upper tail standard normal critical value.

For different values of indexes  $j = 1, \dots, \Gamma(n, d)$ ,  $l = 1, \dots, \Gamma(h, d)$ ,  $n, h \in \mathbb{N}_0$ , different Gaussian random directions in  $\mathcal{S}(L^2(\mathbb{M}_d, d\nu; \mathbb{C}))$  can be defined from

$$\mathbf{k}_{n,j,h,l}(\tau, \sigma) = Y_{n,j,h,l} [S_{n,j}^d \otimes \overline{S_{h,l}^d}(\tau, \sigma)], \quad (\tau, \sigma) \in \mathbb{M}_d^2, \quad (41)$$

where  $Y_{n,j,h,l}$  denotes a zero-mean Gaussian random variable with variance  $\lambda_{n,j,h,l}$ . These random directions a.s. satisfy the eigenequation associated with the Laplace–Beltrami operator on  $\mathbb{M}_d$  (see also [17] on Gaussian random spherical harmonics). The Gaussian random directions involved in the eigenspaces where stronger persistent in time is displayed play a key role in this testing procedure. Furthermore, if we assume that  $\sum_{n \in \mathbb{N}_0} \sum_{h \in \mathbb{N}_0} \sum_{j=1}^{\Gamma(n,d)} \sum_{l=1}^{\Gamma(h,d)} \lambda_{n,j,h,l} < \infty$ , Lemma 4 provides a way to generate  $\mathbf{k}$  from the Karhunen–Loève expansion. That is, one can consider  $\mathbf{k}$  to be a zero-mean Gaussian random element in  $\mathcal{S}(L^2(\mathbb{M}_d, d\nu; \mathbb{C}))$  satisfying (28), with covariance operator  $\mathcal{C}_{\mathbf{k}}$  having covariance kernel

$$\begin{aligned} C_{\mathbf{k}}(\tau_1, \sigma_1, \tau_2, \sigma_2) &= E[\mathbf{k}(\tau_1, \sigma_1) \mathbf{k}(\tau_2, \sigma_2)] \\ &= \sum_{n \in \mathbb{N}_0} \sum_{j=1}^{\Gamma(n,d)} \sum_{h \in \mathbb{N}_0} \sum_{l=1}^{\Gamma(h,d)} \lambda_n \lambda_h \left[ S_{n,j}^d(\tau_1) \overline{S_{h,l}^d}(\sigma_1) S_{n,j}^d(\tau_2) \overline{S_{h,l}^d}(\sigma_2) \right. \\ &\quad \left. + S_{n,j}^d(\tau_1) \overline{S_{h,l}^d}(\sigma_1) \overline{S_{h,l}^d}(\tau_2) S_{n,j}^d(\sigma_2) \right], \quad \forall (\tau_1, \sigma_1), (\tau_2, \sigma_2) \in \mathbb{M}_d^2. \quad (42) \end{aligned}$$

The large functional sample size properties of  $\mathcal{S}_{B_T}$  are numerically illustrated in the next section by simulations, paying special attention to the illustration of Theorems 1 and 3. Robust empirical sizes, and good empirical power properties are observed.

## 5 Simulation study

Our simulations will be set on  $\mathbb{M}_d = \mathbb{S}_d \subset \mathbb{R}^{d+1}$ . Theorem 1 is illustrated in the context of SPHARMA(p,q) processes, and the illustration of Theorem

3 is carried out in the context of multifractionally integrated SPHARMA(p,q) process. An alternative generation algorithm to the ones considered in [18] and [19] is implemented reducing computational burden allowing for the consideration of large functional sample sizes. The results are reported in Sections 5.1 and 5.2 for  $\beta = 1/4$ , i.e.,  $B_T = T^{-1/4}$ . A final summary of the results for different  $\beta$  values is also provided for discussion in Section 6.

## 5.1 Asymptotic Gaussian distribution of $\mathcal{S}_{B_T}$ under $H_0$

Let us consider that the elements of the family of spectral density operators of  $X$  have frequency varying eigenvalues, with respect to the system of eigenfunctions of the Laplace–Beltrami operator, obeying the following equation under  $H_0$  (see [28]):

$$f_n(\omega) = \frac{\lambda_n(\mathcal{R}_0^n)}{2\pi} \left| \frac{\Psi_{q,n}(\exp(-i\omega))}{\Phi_{p,n}(\exp(-i\omega))} \right|^2, \quad n \in \mathbb{N}_0, \quad (43)$$

where  $\{\lambda_n(\mathcal{R}_0^n), n \in \mathbb{N}_0\}$  is the system of eigenvalues of the autocovariance operator  $\mathcal{R}_0^n$  of the innovation process  $\eta = \{\eta_t, t \in \mathbb{Z}\}$  which is assumed to be strong–white noise in  $L^2(\mathbb{S}_d, d\nu, \mathbb{R})$ . That is,  $\eta = \{\eta_t, t \in \mathbb{Z}\}$  is assumed to be a sequence of independent and identically distributed  $L^2(\mathbb{S}_d, d\nu, \mathbb{R})$ –valued random variables such that  $E[\eta_t] = 0$ , and  $E[\eta_t \otimes \eta_s] = \delta_{t,s} \mathcal{R}_0^n$ , with  $\mathcal{R}_0^n \in L^1(L^2(\mathbb{S}_d, d\nu, \mathbb{R}))$ , and  $\delta_{t,s} = 0$ , for  $t \neq s$ , and  $\delta_{t,s} = 1$ , for  $t = s$ . For  $n \in \mathbb{N}_0$ ,  $\Phi_{p,n}(z) = 1 - \sum_{j=1}^p \lambda_n(\varphi_j) z^j$  and  $\Psi_{q,n} = \sum_{j=1}^q \lambda_n(\psi_j) z^j$ , with  $\{\lambda_n(\varphi_j), n \in \mathbb{N}_0\}$  and  $\{\lambda_n(\psi_l), n \in \mathbb{N}_0\}$  denoting the sequences of eigenvalues, with respect to the system of eigenfunctions of the Laplace–Beltrami operator, of the self–adjoint invariant integral operators  $\varphi_j$  and  $\psi_l$ , for  $j = 1, \dots, p$ , and  $l = 1, \dots, q$ , respectively. These operators satisfy the following equations:

$$\Phi_p(B) = 1 - \sum_{j=1}^p \varphi_j B^j, \quad \Psi_q(B) = \sum_{j=1}^q \psi_j B^j,$$

where  $B$  is a difference operator such that

$$E\|B^j X_t - X_{t-j}\|_{L^2(\mathbb{S}_d, d\nu, \mathbb{R})}^2 = 0, \quad \forall t, j \in \mathbb{Z}. \quad (44)$$

Here,  $\Phi_p$  and  $\Psi_q$  are the so–called autoregressive and moving average operators, respectively. Also, for each  $n \in \mathbb{N}_0$ ,  $\Phi_{p,n}(z) = 1 - \sum_{j=1}^p \lambda_n(\varphi_j) z^j$  and  $\Psi_{q,n} = \sum_{j=1}^q \lambda_n(\psi_j) z^j$  have not common roots, and their roots are outside of the unit circle (see also Corollary 6.17 in [1]). Thus,  $X$  satisfies an SPHARMA(p,q) equation (see, e.g., [2]).

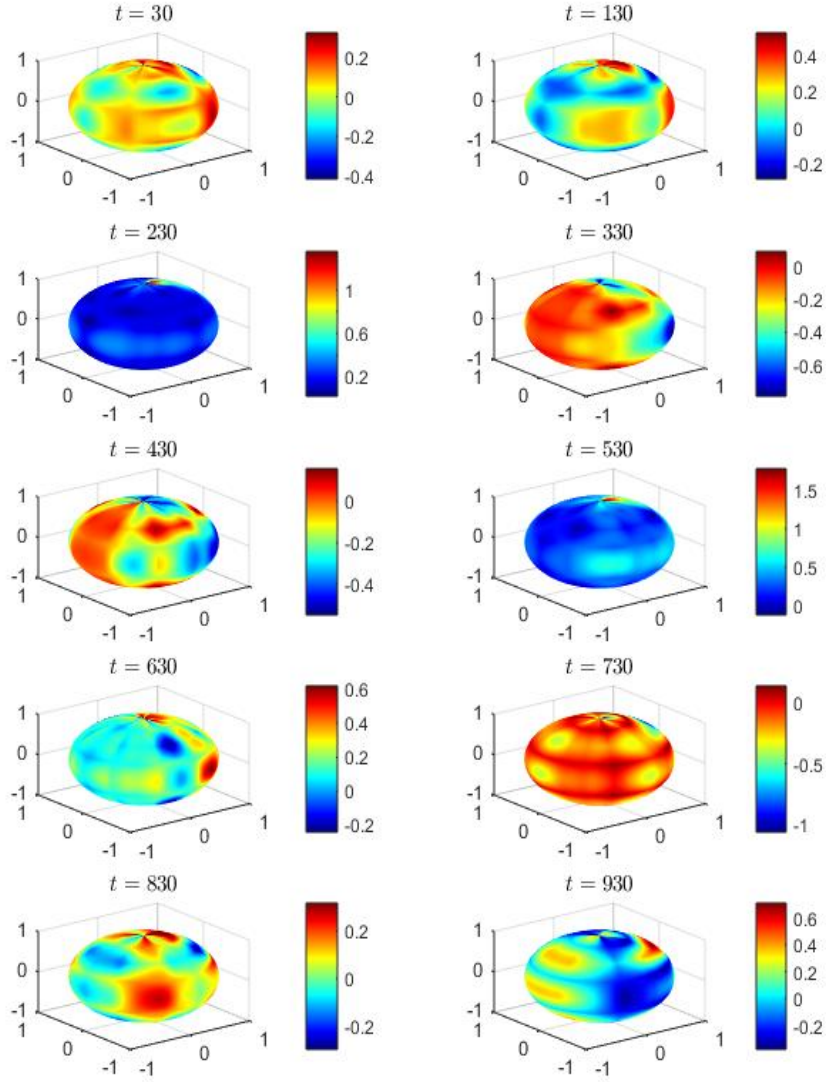


Figure 1: One realization at times  $t = 30, 130, 230, 330, 430, 530, 630, 730, 830, 930$  of SPHARMA(1,1) process  $(\lambda_n(\varphi_1) = 0.7 \left(\frac{n+1}{n}\right)^{-3/2}$ , and  $\lambda_n(\psi_1) = (0.4) \left(\frac{n+1}{n}\right)^{-5/1.95}$ ,  $n = 1, 2, 3, 4, 5, 6, 7, 8$ ), projected into the direct sum  $\bigoplus_{n=1}^8 \mathcal{H}_n$  of eigenspaces  $\mathcal{H}_n$ ,  $n = 1, \dots, 8$ , of  $\Delta_2$

In the simulations we have generated SPHARMA(1,1) process, i.e.,  $p = q = 1$ , with  $H = L^2(\mathbb{S}_2, d\nu, \mathbb{R})$ , and  $\lambda_n(\varphi_1) = 0.7 \left(\frac{n+1}{n}\right)^{-3/2}$  and  $\lambda_n(\psi_1) = (0.4) \left(\frac{n+1}{n}\right)^{-5/1.95}$ ,  $n \in \mathbb{N}_0$ . Figure 1 displays one realization of the generated SPHARMA(1,1) process projected into  $\bigoplus_{n=1}^8 \mathcal{H}_n$ , at times  $t = 30, 130, 230, 330, 430, 530, 630, 730, 830, 930$ .

The empirical distribution of the centered and standardized projections of  $\mathcal{S}_{B_T}$  into  $\mathcal{H}_n \otimes \mathcal{H}_n$ , for each  $n = 1, \dots, 8$ , are displayed for functional sample size  $T = 1000$  and  $R = 3000$  repetitions in Figure 2, for functional sample size  $T = 2000$  and  $R = 3000$  repetitions in Figure 3, and for functional sample size  $T = 3000$  and  $R = 3000$  repetitions in Figure 4. These empirical distributions approximate the support and shape of a standard Gaussian probability density. The empirical standardization displays a decreasing pattern over the spherical scale  $n$ , meaning that the respective limit one-dimensional Gaussian probability measures of these projections have decreasing support (see Figures 2–4). According to Theorem 1.2.1 in [6], this property is satisfied by the infinite product Gaussian measure on  $(\mathbb{R}^\infty, \mathcal{B}(\mathbb{R}^\infty))$ , whose restriction to  $L^2(\mathbb{S}_d, d\nu, \mathbb{R})$  is identified in the  $\ell^2$ -sense with the probability measure of the limit Gaussian random element in Lemma 1.

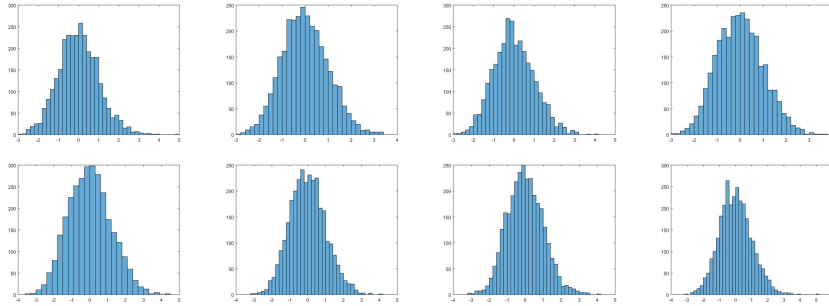


Figure 2: Empirical projections of the probability measure of standardized  $\mathcal{S}_{B_T}$ ,  $B_T = T^{-1/4}$ , under  $H_0$ , into the eigenspaces  $\mathcal{H}_n \otimes \mathcal{H}_n$ , for  $n = 1, 2, 3, 4, 5, 6, 7, 8$ , respectively displayed from the left to the right, and from the top to the bottom, for functional samples size  $T = 1000$  and  $R = 3000$  repetitions

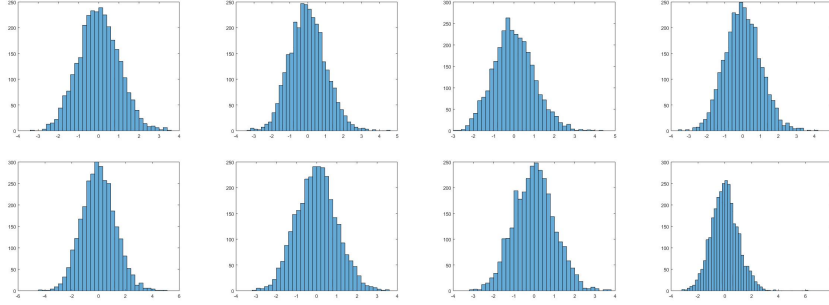


Figure 3: Empirical projections of the probability measure of standardized  $\mathcal{S}_{B_T}$ ,  $B_T = T^{-1/4}$ , under  $H_0$ , into the eigenspaces  $\mathcal{H}_n \otimes \mathcal{H}_n$ , for  $n = 1, 2, 3, 4, 5, 6, 7, 8$ , respectively displayed from the left to the right, and from the top to the bottom, for functional samples size  $T = 2000$  and  $R = 3000$  repetitions

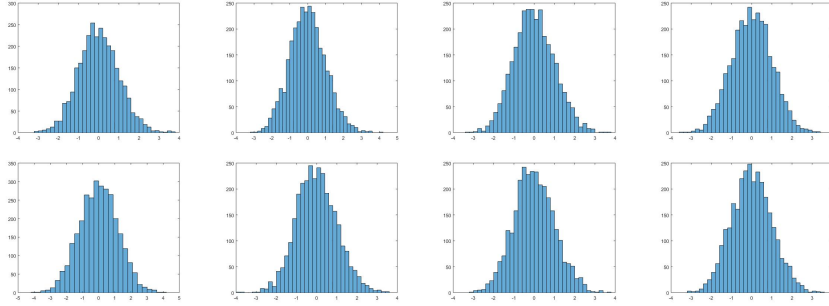


Figure 4: Empirical projections of the probability measure of standardized  $\mathcal{S}_{B_T}$ ,  $B_T = T^{-1/4}$ , under  $H_0$ , into the eigenspaces  $\mathcal{H}_n \otimes \mathcal{H}_n$ , for  $n = 1, 2, 3, 4, 5, 6, 7, 8$ , respectively displayed from the left to the right, and from the top to the bottom, for functional samples size  $T = 3000$  and  $R = 3000$  repetitions

## 5.2 Consistency of the test

Under  $H_1$ , for each  $\omega \in [-\pi, \pi]$ , the eigenvalues  $\{f_n(\omega), n \in \mathbb{N}_0\}$  satisfy (see equations (17)–(18))

$$f_n(\omega) = \frac{\lambda_n(\mathcal{R}_0^\eta)}{2\pi} \left| \frac{\Psi_{q,n}(\exp(-i\omega))}{\Phi_{p,n}(\exp(-i\omega))} \right|^2 |1 - \exp(-i\omega)|^{-\alpha(n)}, \quad n \in \mathbb{N}_0. \quad (45)$$

Again, we consider the projection of  $X$  into  $\bigoplus_{n=1}^8 \mathcal{H}_n$ . Three multifractional integration operators, applied to SPHARMA(1,1) process generated in Section 5.1, are considered in Sections 5.2.1–5.2.3. In Example 1,  $\alpha(n)$  is decreasing over  $n$ , in Example 2 is increasing, and non-monotone in Example 3. The figures of Sections 5.2.1–5.2.3 are displayed in Section D of the Appendices.

### 5.2.1 Example 1

Theorem 3 is now illustrated in the case where the largest dependence range is displayed by the process projected into the eigenspace  $\mathcal{H}_1$ . Figure 5 displays a sample realization of multifractionally integrated SPHARMA (1,1) process  $X$  projected into  $\bigoplus_{i=1}^8 \mathcal{H}_i$ , for  $L_\alpha = 0.4733$ , and  $l_\alpha = 0.2678$ , and  $\alpha(n) = l_\alpha = 0.2678$ ,  $n \geq 9$  (see Figure 6). The a.s. divergence of  $\mathcal{S}_{B_T}$ , for  $B_T = T^{-1/4}$ , in the Hilbert–Schmidt operator norm (see Table 1) is also reflected in the observed increasing sample values of each one of its projections into  $\mathcal{H}_n \otimes \mathcal{H}_n$ ,  $n = 1, \dots, 8$ , for the increasing functional samples sizes  $T = 1000, 10000, 30000$  (see Figure 7).

### 5.2.2 Example 2

The dominant subspace in this example, where the projected process displays the largest dependence range, is eigenspace  $\mathcal{H}_8$ . One sample realization of the generated multifractionally integrated SPHARMA (1,1) process, projected into  $\bigoplus_{n=1}^8 \mathcal{H}_n$ , is displayed in Figure 8. The LRD operator eigenvalues  $\alpha(n)$ ,  $n = 1, 2, 3, 4, 5, 6, 7, 8$ , are plotted in Figure 9, with  $L_\alpha = 0.3327$ , and  $l_\alpha = 0.2550$ , with  $\alpha(n) = l_\alpha = 0.2550$ ,  $n \geq 9$ . The a.s. divergence of our test statistics operator in the Hilbert–Schmidt operator norm (see also Table 1) is illustrated in Figure 10, in terms of the sample values of each projection of  $\mathcal{S}_{B_T}$ ,  $B_T = T^{-1/4}$ , into  $\mathcal{H}_n \otimes \mathcal{H}_n$ , for  $n = 1, \dots, 8$ , and for functional samples sizes  $T = 1000, 10000, 30000$ .

### 5.2.3 Example 3

In this third example, the dominant subspace is eigenspace  $\mathcal{H}_5$  of the Laplace–Beltrami operator. One sample realization of the generated multifractionally integrated SPHARMA (1,1) process, projected into  $\bigoplus_{n=1}^8 \mathcal{H}_n$ , is displayed in Figure 11. The eigenvalues  $\alpha(n)$ ,  $n = 1, 2, 3, 4, 5, 6, 7, 8$ , of LRD operator  $\mathcal{A}$  are plotted in Figure 12, where  $L_\alpha = 0.4000$ , and  $l_\alpha = 0.2753 = \alpha(n)$ ,  $n \geq 9$ . Figure 13 shows the sample values of the projections of  $\mathcal{S}_{B_T}$ ,  $B_T = T^{-1/4}$ , into  $\mathcal{H}_n \otimes \mathcal{H}_n$ , for each  $n = 1, \dots, 8$ , and functional samples sizes  $T = 1000, 10000, 30000$  (see also Table 1).

### 5.2.4 Almost surely divergence of $\mathcal{S}_{B_T}$ in $\mathcal{S}(L^2(\mathbb{M}_d, d\nu, \mathbb{C}))$ norm under $H_1$

The Hilbert-Schmidt operator norm of  $\mathcal{S}_{B_T}$ , for  $B_T = T^{-1/4}$ , projected into  $\bigoplus_{n=1}^8 \mathcal{H}_n \otimes \mathcal{H}_n$ , is displayed in Table 1, for the three numerical examples analyzed, and for the functional sample sizes (F.S.Ss)  $T = 1000, 5000, 10000, 30000, 50000, 100000$ .

One can observe in Table 1 the increasing sample values of the Hilbert–Schmidt

Table 1: *Hilbert-Schmidt operator norm of projected  $\mathcal{S}_{B_T}$ ,  $\beta = 1/4$*

F.S.S.	Example 1	Example 2	Example 3
$T = 1000$	2.3036e+05	2.2595e+05	1.9934e+05
$T = 5000$	1.0612e+07	1.0223e+07	9.0697e+06
$T = 10000$	5.5172e+07	5.3770e+07	4.7303e+07
$T = 30000$	7.5695e+08	7.3377e+08	6.4742e+08
$T = 50000$	2.5516e+09	2.4764e+09	2.1844e+09
$T = 100000$	1.3256e+10	1.2892e+10	1.2906e+10

operator norm of the projected  $\mathcal{S}_{B_T}$  as  $T$  increases, in all the examples under  $l_\alpha > 1/4$ , with  $B_T = T^{-\beta}$ ,  $\beta = 1/4$ , satisfying  $TB_T \rightarrow \infty$ ,  $T \rightarrow \infty$ . Spherical sample patterns and scales induced by the multifractional integration operator (see Figures 5, 8 and 11) have no significant effect (see Table 1), when the condition  $l_\alpha > 1/4$  is satisfied under the bandwidth parameter modelling  $B_T = T^{-\beta}$ ,  $\beta \in (0, 1)$ . This fact is also reflected in Figures 7, 10 and 13, where decreasing patterns are displayed by the sample values of  $\mathcal{S}_{B_T}$  projected into  $\mathcal{H}_n \otimes \mathcal{H}_n$  over  $n = 1, 2, 3, 4, 5, 6, 7, 8$ , in all the examples. However, the scenario under which  $\alpha(n)$  crosses the threshold  $1/2$  at some spherical scale  $n$  requires a separated analysis, as briefly discuss in Example 4 in the next section (see Figures 15–16 in Section D.1.4 of the Appendices).

### 5.3 Example 4

Our numerical analysis is slightly extended here beyond the restriction  $L_\alpha > 1/2$ . Specifically, this section shows some preliminary numerical results regarding the effect of higher levels of singularity at zero frequency when  $L_\alpha > 1/2$ , i.e.,  $\|\mathcal{A}\|_{\mathcal{L}(L^2(\mathbb{S}_2, d\nu, \mathbb{R}))} > 1/2$ , corresponding to a stronger persistent in time of the projected process into the dominant subspace (see Figure 14 in Section D.1.4 of the Appendices). Under this scenario, conditions (16), and (37) in Theorem 2 are not satisfied. Indeed, we are outside of the scenario where the summability in time of the square of the Hilbert–Schmidt operator norms of the elements of the covariance operator family holds. Then, new technical tools are required to address the asymptotic analysis in the spectral domain of this family of manifold supported functional time series displaying stronger levels of persistent in time.

Let us again consider  $\mathcal{S}_{B_T}$ , for  $B_T = T^{-1/4}$ , projected into  $\bigoplus_{n=1}^8 \mathcal{H}_n \otimes \mathcal{H}_n$ . In this example, the multifractional integration of SPHARMA(1,1) process

generated in Section 5.1 has been achieved in terms of LRD operator  $\mathcal{A}$  having eigenvalues displayed in Figure 15 in Section D.1.4 of the Appendices, with  $L_\alpha = 0.9982$  and  $l_\alpha = 0.3041$ , and  $\mathcal{H}_8$  being the dominant subspace. The same functional sample sizes as in Examples 1–3 have been considered. One can observe in Figure 16 in Section D.1.4 of the Appendices, that the decreasing patterns over  $n = 1, \dots, 8$ , displayed in Figures 7, 10 and 13 (see Sections D.1.1–D.1.3 of the Appendices) do not hold in this example. Table 2 also illustrates a faster increasing than in Examples 1–3 of  $\|\mathcal{S}_{B_T}\|_{\mathcal{S}(L^2(\mathbb{M}_d, d\nu, \mathbb{C}))}$ , for functional sample sizes  $T = 1000, 5000, 10000, 30000, 50000$ , under  $l_\alpha > 1/4$ , and  $B_T = T^{-1/4}$ .

Table 2: *Hilbert-Schmidt operator norm of projected  $\mathcal{S}_{B_T}$*  ( $\beta = 1/4$ ,  $L_\alpha = 0.9982$  and  $l_\alpha = 0.3041$ )

F.S.S.	Example 4
$T = 1000$	6.5651e+05
$T = 5000$	3.8623e+07
$T = 10000$	2.2172e+08
$T = 30000$	3.5383e+09
$T = 50000$	1.2688e+10
$T = 100000$	7.2258e+10

## 5.4 Empirical size and power based analysis

The empirical size and power properties of the testing approach presented are now illustrated. We have applied random projection methodology. Tables 3 and 4 display the numerical results for 8 random functional directions, i.e., equation (40) is implemented including  $\mathbf{k}_{1,0,1,0}$ ,  $\mathbf{k}_{1,1,1,1}$ ,  $\mathbf{k}_{2,1,2,1}$ ,  $\mathbf{k}_{2,2,2,2}$ ,  $\mathbf{k}_{3,1,3,1}$ ,  $\mathbf{k}_{3,2,3,2}$ ,  $\mathbf{k}_{3,3,3,3}$ , defined in (41). Model SPHARMA(1,1) generated in Section 5.1 has been considered in the computation of the empirical size of the test. Multifractionally integrated SPHARMA(1,1) model, generated in Section 5.2.1, defines the scenario under the alternative to compute the empirical power. For each one of the eight random directions tested, we have analyzed the functional samples sizes  $T = 50, 100, 500, 1000$ , and, for each functional sample size, we have considered  $R = 500, 1000, 3000$  repetitions.

The empirical size properties of the proposed test procedure are quite robust (see numerical results in Table 3), regarding the estimated size  $\hat{\alpha}$ , from each one of the  $T$  values analyzed when different values of  $R$  are considered. One can also



observe, in Table 4, the increasing patterns displayed by the empirical power with respect to the functional sample sizes tested in all random directions. Note that these empirical power values lye in the interval  $[0.776, 1]$ . In particular, since the threshold  $T = 1000$ , the empirical power is almost 1 for any of the three values of  $R$  studied.

Table 3: *Empirical size* ( $\beta = 1/4$ ,  $\mathbf{k}_{n,j,h,l}$ ,  $n = h = 1, 2, 3$ ,  $\alpha = 0.05$ )

$R = 500, T = 50$							
0.0280	0.0560	0.0360	0.0480	0.0600	0.0600	0.0360	0.0520
$R = 1000, T = 50$							
0.0480	0.0420	0.0320	0.0380	0.0420	0.0440	0.0320	0.0300
$R = 3000, T = 50$							
0.0420	0.0447	0.0453	0.0353	0.0413	0.0400	0.0440	0.0507
$R = 500, T = 100$							
0.0360	0.0680	0.0440	0.0720	0.0520	0.0240	0.0360	0.0400
$R = 1000, T = 100$							
0.0280	0.0380	0.0380	0.0500	0.0380	0.0740	0.0340	0.0360
$R=3000,T=100$							
0.0373	0.0507	0.0407	0.0460	0.0440	0.0360	0.0600	0.0480
$R=500,T=500$							
0.0440	0.0520	0.0320	0.0640	0.0320	0.0480	0.0320	0.0480
$R=1000,T=500$							
0.0420	0.0400	0.0500	0.0460	0.0420	0.0380	0.0540	0.0240
$R=3000,T=500$							
0.0453	0.0393	0.0447	0.0407	0.0427	0.0507	0.0453	0.0553
$R=500,T=1000$							
0.0520	0.0360	0.0400	0.0560	0.0600	0.0640	0.0480	0.0520
$R=1000,T=1000$							
0.0440	0.0380	0.0400	0.0580	0.0500	0.0360	0.0520	0.0400
$R=3000,T=1000$							
0.0573	0.0480	0.0507	0.0467	0.0440	0.0453	0.0487	0.0447

## 6 Final comments and discussion

The simulation study illustrates three key aspects of our approach:

Table 4: *Empirical power* ( $\beta = 1/4$ ,  $\mathbf{k}_{n,j,h,l}$ ,  $n = h = 1, 2, 3$ ,  $\alpha = 0.05$ )

$R = 500, T = 50$							
0.9200	0.9240	0.8640	0.8880	0.8480	0.8160	0.7760	0.7800
$R = 1000, T = 50$							
0.9000	0.9000	0.8860	0.8980	0.8000	0.8320	0.7840	0.7840
$R = 3000, T = 50$							
0.9247	0.9253	0.8713	0.8760	0.8247	0.8273	0.7980	0.8013
$R = 500, T = 100$							
0.9920	0.9920	0.9920	0.9880	0.9840	0.9800	0.9880	0.9720
$R = 1000, T = 100$							
0.9880	0.9880	0.9860	0.9840	0.9800	0.9720	0.9740	0.9840
$R=3000,T=100$							
0.9893	0.9893	0.9920	0.9827	0.9820	0.9773	0.9767	0.9747
$R=500,T=500$							
1.0000	1.0000	1.0000	0.9960	1.0000	0.9960	1.0000	1.0000
$R=1000,T=500$							
1.0000	1.0000	1.0000	1.0000	0.9980	1.0000	0.9980	1.0000
$R=3000,T=500$							
1.0000	0.9987	1.0000	1.0000	0.9993	1.0000	0.9993	0.9993
$R=500,T=1000$							
1	1	1	1	1	1	1	1
$R=1000,T=1000$							
1	1	1	1	1	1	1	1
$R=3000,T=1000$							
1	1	1	1	1	1	1	1

- (i) The tight property of the scaled and centered weighted periodogram operator under  $H_0$ , allowing the application of Prokhorov Theorem to prove the convergence of  $\mathcal{S}_{B_T}$  to  $\widehat{\mathcal{F}}_0$ , as  $T \rightarrow \infty$ , in the space  $\mathcal{L}_{\mathcal{S}(L^2(\mathbb{M}_d, d\nu, \mathbb{C}))}^2(\Omega, \mathcal{A}, P)$ , from Dominated Convergence Theorem. In particular, the asymptotic Gaussian distribution of  $\mathcal{S}_{B_T}$  under  $H_0$  follows. This result is illustrated in Section 5.1 from Theorem 1.2.1 in [6].
- (ii) The crucial role played by our design of the test statistics operator in the derivation of the conditions assumed to obtain consistency (see Proposition 1 and Theorem 2). The simulation study also reveals that the additional conditions assumed in Theorem 3 lead to an universal divergence rate, not

affected by the localization of the dominant eigenspace, or the value of the parameter  $\beta \in (0, 1)$  chosen, under the bandwidth parameter scenario  $B_T = T^{-\beta}$  when  $l_\alpha > 1/4$ .

- (iii) The testing approach adopted displays good empirical size and power properties for finite functional sample sizes, as displayed in Tables 3 and 4, when  $\mathcal{S}_{B_T}$  satisfies Carleman condition.

Regarding topic (ii), our final conclusions are supported by the numerical results showed in Table 5, where, in the three examples analyzed, for large functional sample sizes  $T = 1000, 50000, 100000$ , the sample values of  $\left\| \frac{\mathcal{S}_{B_T}}{(TB_T)^{1/2}} \right\|_{\mathcal{S}(L^2(\mathbb{M}_d, d\nu, \mathbb{C}))}$  are displayed, when  $\mathcal{S}_{B_T}$  is projected into  $\bigoplus_{n=1}^8 \mathcal{H}_n \otimes \mathcal{H}_n$ , and  $\beta = 0.2, 0.55, 0.9$ .

Table 5:  $\left\| \frac{\mathcal{S}_{B_T}}{(TB_T)^{1/2}} \right\|_{\mathcal{S}(L^2(\mathbb{M}_d, d\nu, \mathbb{C}))}$ ,  $\mathcal{S}_{B_T}$  projected into  $\bigoplus_{n=1}^8 \mathcal{H}_n \otimes \mathcal{H}_n$

	<b>F.S.S.</b>	<b>Example 1</b>	<b>Example 2</b>	<b>Example 3</b>
$\beta = 0.2$	$T = 1000$	1.6885(1.0e+04)	1.6384(1.0e+04)	1.6438(1.0e+04)
	$T = 50000$	4.3549(1.0e+07)	4.2251(1.0e+07)	4.2290(1.0e+07)
	$T = 100000$	1.7493(1.0e+08)	1.6944(1.0e+08)	1.6989(1.0e+08)
$\beta = 0.55$	$T = 1000$	1.8067 (1.0e+04)	1.7733(1.0e+04)	1.7693(1.0e+04)
	$T = 50000$	4.4789(1.0e+07)	4.3747(1.0e+07)	4.3510(1.0e+07)
	$T = 100000$	1.7984(1.0e+08)	1.7470(1.0e+08)	1.7476(1.0e+08)
$\beta = 0.9$	$T = 1000$	2.0296(1.0e+04)	2.0109(1.0e+04)	1.9993(1.0e+04)
	$T = 50000$	4.5133(1.0e+07)	4.4271(1.0e+07)	4.4138(1.0e+07)
	$T = 100000$	1.8040 (1.0e+08)	1.7518(1.0e+08)	1.7624(1.0e+08)

Although, as expected, the sample values of  $\left\| \frac{\mathcal{S}_{B_T}}{(TB_T)^{1/2}} \right\|_{\mathcal{S}(L^2(\mathbb{M}_d, d\nu, \mathbb{C}))}$  slightly increase when  $\beta$  increases in Examples 1–3, no significant differences are observed in the sample divergence rate of  $\left\| \frac{\mathcal{S}_{B_T}}{(TB_T)^{1/2}} \right\|_{\mathcal{S}(L^2(\mathbb{M}_d, d\nu, \mathbb{C}))}$ , for the three values of parameter  $\beta$  analyzed in Table 5 (see the proof of Theorem 3). Furthermore, as proved in Theorem 3, under condition  $l_\alpha > 1/4$ , when  $B_T = T^{-\beta}$ ,  $\beta \in (0, 1)$ , one can also observe that the location of the dominant eigenspace does not affect the sample divergence rate. Note also that, as illustrated in [18], the regular spectral factor  $\mathcal{M}_\omega$ , corresponding here to the SPHARMA(p,q) functional spectrum, has not effect in the asymptotic analysis when its multifractionally integration is considered.

## Acknowledgements

This work has been supported in part by projects PID2022–142900NB-I00 and PID2020-116587GB-I00, financed by MCIU/AEI/10.13039/501100011033 and by FEDER UE, and CEX2020-001105-M MCIN/AEI/10.13039/501100011033), as well as supported by grant ED431C 2021/24 (Grupos competitivos) financed by Xunta de Galicia through European Regional Development Funds (ERDF).

## Appendices

The proofs of the results of the paper are given in the subsequent sections.

## A Proofs for Section 2

### A.1 Proof of Lemma 4

**Proof.** For  $\omega \in [-\pi, \pi]$ , denote by  $\widehat{\mathcal{F}}_\omega$  the limit Gaussian random operator with kernel  $\widehat{f}_\omega$  introduced in Lemma 3. Let us consider the orthonormal basis

$$\left\{ S_{n,j}^d \otimes \overline{S_{h,l}^d}, \overline{S_{h,l}^d} \otimes S_{n,j}^d \right\}_{j=1, \dots, \Gamma(n,d), l=1, \dots, \Gamma(h,d); n, h \in \mathbb{N}_0}. \quad (46)$$

From equations (2) and (26), for every  $(\tau_i, \sigma_i) \in \mathbb{M}_d^2, i = 1, 2, \omega, \xi \in [-\pi, \pi]$ , the kernel of the cross covariance operator  $\mathcal{R}_{\widehat{\mathcal{F}}_\omega, \widehat{\mathcal{F}}_\xi} = E \left[ \widehat{\mathcal{F}}_\omega \otimes \widehat{\mathcal{F}}_\xi \right]$  admits the following series expansion:

$$\begin{aligned} & \frac{1}{\|W\|_{L^2(\mathbb{R})}^2} E \left[ \widehat{f}_\omega \otimes \widehat{f}_\xi \right] (\tau_1, \sigma_1, \tau_2, \sigma_2) \\ & \left[ \eta(\omega - \xi) f_\omega(\tau_1, \tau_2) \overline{f_\omega(\sigma_1, \sigma_2)} + \eta(\omega + \xi) f_\omega(\tau_1, \sigma_2) \overline{f_\omega(\sigma_1, \tau_2)} \right] \\ & = \left[ \sum_{n, h \in \mathbb{N}_0} \sum_{j=1}^{\Gamma(n,d)} \sum_{l=1}^{\Gamma(h,d)} f_n(\omega) f_h(\omega) \left[ \eta(\omega - \xi) \left[ S_{n,j}^d(\tau_1) S_{n,j}^d(\tau_2) \overline{S_{h,l}^d(\sigma_1) S_{h,l}^d(\sigma_2)} \right] \right. \right. \\ & \quad \left. \left. + \eta(\omega + \xi) \left[ S_{n,j}^d(\tau_1) S_{n,j}^d(\sigma_2) \overline{S_{h,l}^d(\sigma_1) S_{h,l}^d(\tau_2)} \right] \right] \right] \\ & = \left[ \sum_{n, h \in \mathbb{N}_0} \sum_{j=1}^{\Gamma(n,d)} \sum_{l=1}^{\Gamma(h,d)} f_n(\omega) f_h(\omega) \left[ \eta(\omega - \xi) \left[ S_{n,j}^d \otimes \overline{S_{h,l}^d}(\tau_1, \sigma_1) S_{n,j}^d \otimes \overline{S_{h,l}^d}(\tau_2, \sigma_2) \right] \right. \right. \\ & \quad \left. \left. + \eta(\omega + \xi) \left[ S_{n,j}^d \otimes \overline{S_{h,l}^d}(\tau_1, \sigma_1) \overline{S_{h,l}^d} \otimes S_{n,j}^d(\tau_2, \sigma_2) \right] \right] \right], \quad (47) \end{aligned}$$

where  $\eta$  has been introduced in (26). The diagonal coefficients are given, for every  $\omega, \xi \in [-\pi, \pi]$ , by

$$\left\{ \lambda_{n,h}^{(\infty)}(\omega, \xi) \right\}_{n,h \in \mathbb{N}_0} = \{ f_n(\omega) f_h(\omega) \eta(\omega - \xi), f_n(\omega) f_h(\omega) \eta(\omega + \xi) \}_{n,h \in \mathbb{N}_0}.$$

In particular, since  $\mathbb{M}_d^2$  is a compact set, and  $\mathcal{R}_{\widehat{\mathcal{F}}_\omega, \widehat{\mathcal{F}}_\omega}$  is a trace nonnegative semidefinite self-adjoint operator, the orthogonal expansion (28) holds in the space  $\mathcal{L}_S(L^2(\mathbb{M}_d, d\nu; \mathbb{C}))(\Omega, \mathcal{A}, \mathcal{P})$ .

## A.2 Proof of Theorem 1

**Proof.** From Theorem D2 in the Supplementary Material of [20], under  $H_0$ , for every  $(\tau_i, \sigma_i) \in \mathbb{M}_d^2$ ,  $i = 1, 2$ , considering (2)

$$\begin{aligned} & \text{cov} \left( \widehat{f}_{\omega_1}^{(T)}(\tau_1, \sigma_1), \widehat{f}_{\omega_2}^{(T)}(\tau_2, \sigma_2) \right) \\ &= \frac{2\pi}{T} \int_{-\pi}^{\pi} W^{(T)}(\omega_1 - \alpha) W^{(T)}(\omega_2 - \alpha) f_\alpha(\tau_1, \tau_2) \overline{f_\alpha(\sigma_1, \sigma_2)} d\alpha \\ &+ \frac{2\pi}{T} \int_{-\pi}^{\pi} W^{(T)}(\omega_1 - \alpha) W^{(T)}(\omega_2 + \alpha) f_\alpha(\tau_1, \sigma_2) \overline{f_\alpha(\sigma_1, \tau_2)} d\alpha \\ &+ \mathcal{O}(B_T^{-2} T^{-2}) + \mathcal{O}(T^{-1}) \\ &= \frac{2\pi}{T} \sum_{n,h \in \mathbb{N}_0} \sum_{j=1}^{\Gamma(n,d)} \sum_{l=1}^{\Gamma(h,d)} \int_{-\pi}^{\pi} W^{(T)}(\omega_1 - \alpha) W^{(T)}(\omega_2 - \alpha) f_n(\alpha) f_h(\alpha) d\alpha \\ &\quad \times S_{n,j}^d(\tau_1) \overline{S_{h,l}^d(\sigma_1)} S_{n,j}^d(\tau_2) \overline{S_{h,l}^d(\sigma_2)} \\ &\quad + \frac{2\pi}{T} \int_{-\pi}^{\pi} W^{(T)}(\omega_1 - \alpha) W^{(T)}(\omega_2 + \alpha) f_n(\alpha) f_h(\alpha) d\alpha \\ &\quad \times S_{n,j}^d(\tau_1) S_{n,j}^d(\sigma_2) \overline{S_{h,l}^d(\sigma_1)} \overline{S_{h,l}^d(\tau_2)} \\ &+ \mathcal{O}(B_T^{-2} T^{-2}) + \mathcal{O}(T^{-1}), \end{aligned} \tag{48}$$

in the  $L^2$  sense and uniformly in  $\omega_i \in [-\pi, \pi]$ ,  $i = 1, 2$ .

From Lemma 3,

$$\sqrt{B_T T} (\widehat{f}_{\omega_j}^{(T)} - E[\widehat{f}_{\omega_j}^{(T)}]) \rightarrow_D \widehat{f}_{\omega_j}, \quad j = 1, \dots, J.$$

Furthermore, from (48), for every  $j = 1, \dots, \Gamma(n, d)$ ,  $n \in \mathbb{N}_0$ , and  $l = 1, \dots, \Gamma(h, l)$ ,  $h \in \mathbb{N}_0$ , and for every  $T \geq T_0$ , for  $T_0$  sufficiently large, the following inequalities

hold:

$$\begin{aligned}
& E \left[ \left| \left\langle \sqrt{B_T T} (\widehat{f}_\omega^{(T)} - E[\widehat{f}_\omega^{(T)}]), S_{n,j}^d \otimes \overline{S_{h,l}^d} \right\rangle_{\mathcal{S}(L^2(\mathbb{M}_d, d\nu, \mathbb{C}))} \right|^2 \right] \\
&= \int_{-\pi}^{\pi} W \left( \frac{\omega - \alpha}{B_T} \right) W \left( \frac{\omega - \alpha}{B_T} \right) f_n(\alpha) f_h(\alpha) \frac{d\alpha}{B_T} \\
&\quad + \mathcal{O}(B_T^{-2} T^{-2}) + \mathcal{O}(T^{-1}) \\
&\leq \| \mathcal{F}_\omega \|_{L^1(\mathcal{S}(L^2(\mathbb{M}_d, d\nu, \mathbb{C})))}^2 + \varepsilon < \infty, \quad \varepsilon > 0, \omega \in [-\pi, \pi] \\
& E \left[ \left| \left\langle \sqrt{B_T T} (\widehat{f}_\omega^{(T)} - E[\widehat{f}_\omega^{(T)}]), \overline{S_{h,l}^d} \otimes S_{n,j}^d \right\rangle_{\mathcal{S}(L^2(\mathbb{M}_d, d\nu, \mathbb{C}))} \right|^2 \right] \\
&= \int_{-\pi}^{\pi} W \left( \frac{\omega - \alpha}{B_T} \right) W \left( \frac{\omega + \alpha}{B_T} \right) f_n(\alpha) f_h(\alpha) \frac{d\alpha}{B_T} \\
&\quad + \mathcal{O}(B_T^{-2} T^{-2}) + \mathcal{O}(T^{-1}) \\
&\leq \| \mathcal{F}_\omega \|_{L^1(\mathcal{S}(L^2(\mathbb{M}_d, d\nu, \mathbb{C})))}^2 + \varepsilon < \infty, \quad \varepsilon > 0, \omega \in [-\pi, \pi],
\end{aligned} \tag{49}$$

under SRD in  $H_0$ . Thus, the sequence is tight, where we have applied that, under SRD,

$$\begin{aligned}
\| \mathcal{F}_\omega \|_{L^1(\mathcal{S}(L^2(\mathbb{M}_d, d\nu, \mathbb{C})))} &\leq \sum_{\tau \in \mathbb{Z}} | \exp(-i\omega\tau) | \| \mathcal{R}_\tau \|_{L^1(\mathcal{S}(L^2(\mathbb{M}_d, d\nu, \mathbb{C})))} \\
&= \sum_{\tau \in \mathbb{Z}} \| \mathcal{R}_\tau \|_{L^1(\mathcal{S}(L^2(\mathbb{M}_d, d\nu, \mathbb{C})))} < \infty, \quad \forall \omega \in [-\pi, \pi].
\end{aligned} \tag{50}$$

Hence, the convergence of  $\sqrt{B_T T} (\widehat{f}_\omega^{(T)} - E[\widehat{f}_\omega^{(T)}])$  to  $\widehat{f}_\omega$  in the norm of the space  $\mathcal{L}_{\mathcal{S}(L^2(\mathbb{M}_d, d\nu, \mathbb{C}))}^2(\Omega, \mathcal{A}, P)$  follows from Prokhorov Theorem, where  $\mathcal{L}_{\mathcal{S}(L^2(\mathbb{M}_d, d\nu, \mathbb{C}))}^2(\Omega, \mathcal{A}, P)$  has been introduced in Lemma 4. Define now the random operator sequence  $\{X^{(T)} = \mathcal{S}_{B_T}, T > 0\}$ , and the functional random variable  $X^{(\infty)} = \widehat{\mathcal{F}}_0$ , where  $\widehat{\mathcal{F}}_\omega, \omega \in [-\pi, \pi]$ , is the Gaussian random operator with kernel  $\widehat{f}_\omega$ , limit in distribution of the centered weighted periodogram (see Lemma 3).

Let us now consider the sequence of random Fourier coefficients,

$$\begin{aligned}
X_{n,j,h,l}^{(T)} &= \left\langle X^{(T)}, S_{n,j}^{(d)} \otimes \overline{S_{h,l}^{(d)}} \right\rangle_{\mathcal{S}(L^2(\mathbb{M}_d, d\nu, \mathbb{C}))} \\
\widetilde{X}_{n,j,h,l}^{(T)} &= \left\langle X^{(T)}, \overline{S_{h,l}^{(d)}} \otimes S_{n,j}^{(d)} \right\rangle_{\mathcal{S}(L^2(\mathbb{M}_d, d\nu, \mathbb{C}))} = \overline{X_{h,l,n,j}^{(T)}} \\
X_{n,j,h,l}^{(\infty)} &= \left\langle X^{(\infty)}, S_{n,j}^{(d)} \otimes \overline{S_{h,l}^{(d)}} \right\rangle_{\mathcal{S}(L^2(\mathbb{M}_d, d\nu, \mathbb{C}))} \\
&= \overline{\widetilde{X_{h,l,n,j}^{(\infty)}}},
\end{aligned} \tag{51}$$

for  $j = 1, \dots, \Gamma(n, d)$ ,  $n \in \mathbb{N}_0$ , and  $l = 1, \dots, \Gamma(h, d)$ ,  $h \in \mathbb{N}_0$ . Denote  $\mathcal{S}(\mathcal{S}(L^2(\mathbb{M}_d, d\nu, \mathbb{C}))) \equiv L^2(\mathbb{M}_d^4, \otimes_{i=1}^4 d\nu(x_i), \mathbb{C})$ ,  $\varphi_{n,j,h,l} = S_{n,j}^{(d)} \otimes \overline{S_{h,l}^{(d)}} \otimes S_{n,j}^{(d)} \otimes \overline{S_{h,l}^{(d)}}$ ,  $\overline{\varphi_{n,j,h,l}}^* = S_{n,j}^{(d)} \otimes \overline{S_{h,l}^{(d)}} \otimes \overline{S_{h,l}^{(d)}} \otimes S_{n,j}^{(d)}$ ,  $Y_\omega^{(T)} = \sqrt{B_T T} [\widehat{\mathcal{F}}_\omega^{(T)} - E[\widehat{\mathcal{F}}_\omega^{(T)}]]$ , and  $Y_\omega^{(\infty)} = \widehat{\mathcal{F}}_\omega$ ,  $\omega \in [-\pi, \pi]$ . Let now explicitly compute, for every  $j = 1, \dots, \Gamma(n, d)$ ,  $n \in \mathbb{N}_0$ ,  $l = 1, \dots, \Gamma(h, d)$ ,  $h \in \mathbb{N}_0$ ,

$$\begin{aligned}
& E \left| X_{n,j,h,l}^{(T)} - X_{n,j,h,l}^{(\infty)} \right|^2 \\
&= \int_{\left[\frac{\sqrt{B_T}}{2}, \frac{\sqrt{B_T}}{2}\right]^2} \left\langle E \left[ Y_\omega^{(T)} \otimes \overline{Y_\xi^{(T)}}^* \right], [\varphi_{n,j,h,l} + \overline{\varphi_{n,j,h,l}}^*] \right\rangle_{\mathcal{S}(\mathcal{S}(H))} \frac{d\omega d\xi}{B_T} \\
&\quad - \int_{\left[\frac{\sqrt{B_T}}{2}, \frac{\sqrt{B_T}}{2}\right]^2} \left\langle E \left[ Y_\omega^{(T)} \otimes \overline{Y_\xi^{(\infty)}}^* \right], [\varphi_{n,j,h,l} + \overline{\varphi_{n,j,h,l}}^*] \right\rangle_{\mathcal{S}(\mathcal{S}(H))} \frac{d\omega d\xi}{B_T} \\
&\quad - \int_{\left[\frac{\sqrt{B_T}}{2}, \frac{\sqrt{B_T}}{2}\right]^2} \left\langle E \left[ Y_\omega^{(\infty)} \otimes \overline{Y_\xi^{(T)}}^* \right], [\varphi_{n,j,h,l} + \overline{\varphi_{n,j,h,l}}^*] \right\rangle_{\mathcal{S}(\mathcal{S}(H))} \frac{d\omega d\xi}{B_T} \\
&\quad + \int_{\left[\frac{\sqrt{B_T}}{2}, \frac{\sqrt{B_T}}{2}\right]^2} \left\langle E \left[ Y_\omega^{(\infty)} \otimes \overline{Y_\xi^{(\infty)}}^* \right], [\varphi_{n,j,h,l} + \overline{\varphi_{n,j,h,l}}^*] \right\rangle_{\mathcal{S}(\mathcal{S}(H))} \frac{d\omega d\xi}{B_T}, \tag{52}
\end{aligned}$$

where  $\overline{k}^*$  denotes the conjugate of the kernel  $k$  of the adjoint operator  $\mathcal{K}^*$  of  $\mathcal{K}$ , and  $H = L^2(\mathbb{M}_d, d\nu, \mathbb{C})$ .

Cauchy-Schwartz inequality in  $\mathcal{L}^2(\Omega, \mathcal{A}, P)$ , and the convergence of  $\sqrt{B_T T}(\widehat{f}_\omega^{(T)} - E[\widehat{f}_\omega^{(T)}])$  to  $\widehat{f}_\omega$  in the norm of the space  $\mathcal{L}_{\mathcal{S}(L^2(\mathbb{M}_d, d\nu, \mathbb{C}))}^2(\Omega, \mathcal{A}, P)$  imply the following pointwise convergences hold, for each  $\omega, \xi \in [-\pi, \pi]$ :

$$\begin{aligned}
& \lim_{T \rightarrow \infty} \left\langle E \left[ Y_\omega^{(T)} \otimes \overline{Y_\xi^{(T)}}^* \right], [\varphi_{n,j,h,l} + \overline{\varphi_{n,j,h,l}}^*] \right\rangle_{\mathcal{S}(\mathcal{S}(H))} \\
&= \left\langle E \left[ Y_\omega^{(\infty)} \otimes \overline{Y_\xi^{(\infty)}}^* \right], [\varphi_{n,j,h,l} + \overline{\varphi_{n,j,h,l}}^*] \right\rangle_{\mathcal{S}(\mathcal{S}(H))} \\
& \lim_{T \rightarrow \infty} \left\langle E \left[ Y_\omega^{(T)} \otimes \overline{Y_\xi^{(\infty)}}^* \right], [\varphi_{n,j,h,l} + \overline{\varphi_{n,j,h,l}}^*] \right\rangle_{\mathcal{S}(\mathcal{S}(H))} \\
&= \left\langle E \left[ Y_\omega^{(\infty)} \otimes \overline{Y_\xi^{(\infty)}}^* \right], [\varphi_{n,j,h,l} + \overline{\varphi_{n,j,h,l}}^*] \right\rangle_{\mathcal{S}(\mathcal{S}(H))} \\
& \lim_{T \rightarrow \infty} \left\langle E \left[ Y_\omega^{(\infty)} \otimes \overline{Y_\xi^{(T)}}^* \right], [\varphi_{n,j,h,l} + \overline{\varphi_{n,j,h,l}}^*] \right\rangle_{\mathcal{S}(\mathcal{S}(H))} \\
&= \left\langle E \left[ Y_\omega^{(\infty)} \otimes \overline{Y_\xi^{(\infty)}}^* \right], [\varphi_{n,j,h,l} + \overline{\varphi_{n,j,h,l}}^*] \right\rangle_{\mathcal{S}(\mathcal{S}(H))}, \tag{53}
\end{aligned}$$

for every  $j = 1, \dots, \Gamma(n, d)$ ,  $n \in \mathbb{N}_0$ ,  $l = 1, \dots, \Gamma(h, d)$ ,  $h \in \mathbb{N}_0$ . Furthermore, for  $T \geq 2$ , applying again Cauchy–Schwartz inequality in  $\mathcal{L}^2(\Omega, \mathcal{A}, P)$ , considering  $\omega, \xi \neq 0, \pi$ ,  $j = 1, \dots, \Gamma(n, d)$ ,  $n \in \mathbb{N}_0$ ,  $l = 1, \dots, \Gamma(h, d)$ ,  $h \in \mathbb{N}_0$ ,

$$\begin{aligned}
& \left\langle E \left[ Y_\omega^{(T)} \otimes \overline{Y_\xi^{(T)}}^\star \right], \varphi_{n,j,h,l} \right\rangle_{\mathcal{S}(\mathcal{S}(H))} \\
&= E \left[ \left\langle Y_\omega^{(T)}, S_{n,j}^{(d)} \otimes \overline{S_{h,l}^{(d)}} \right\rangle_{\mathcal{S}(H)} \left\langle \overline{Y_\xi^{(T)}}^\star, S_{n,j}^{(d)} \otimes \overline{S_{h,l}^{(d)}} \right\rangle_{\mathcal{S}(H)} \right] \\
&\leq \sqrt{E \left| \left\langle Y_\omega^{(T)}, S_{n,j}^{(d)} \otimes \overline{S_{h,l}^{(d)}} \right\rangle_{\mathcal{S}(H)} \right|^2 E \left| \left\langle \overline{Y_\xi^{(T)}}^\star, S_{n,j}^{(d)} \otimes \overline{S_{h,l}^{(d)}} \right\rangle_{\mathcal{S}(H)} \right|^2} \\
&\leq \sqrt{f_n(\omega) f_h(\omega) f_n(\xi) f_h(\xi)}. \tag{54}
\end{aligned}$$

The functional upper bound in (54) satisfies, from Cauchy–Schwartz inequality, applying Fourier transform inversion formula,

$$\begin{aligned}
& \int_{[-\pi, \pi]^2} \sqrt{f_n(\omega) f_h(\omega) f_n(\xi) f_h(\xi)} d\omega d\xi \\
&\leq \left[ \int_{[-\pi, \pi]} f_n(\omega) d\omega \right] \left[ \int_{[-\pi, \pi]} f_h(\omega) d\omega \right] \\
&= B_n(0) B_h(0) < \infty, \quad n, h \in \mathbb{N}_0,
\end{aligned}$$

where

$$B_n(t) = \int_{-\pi}^{\pi} \exp(it\omega) f_n(\omega) d\omega, \quad t \in \mathbb{Z}, \quad n \in \mathbb{N}_0. \tag{55}$$

In a similar way, one can obtain the same upper bound as in (54) for the remaining terms of the sequence of functions involved in (53) before taking limit. The cases where  $\omega = \xi = 0$  and  $\omega = \xi = \pi$  can be addressed in a similar way. Note that  $\delta_T(\omega) = \mathbb{I}_{[-\sqrt{B_T}/2, \sqrt{B_T}/2]}(\omega) / \sqrt{B_T}$  behaves as a truncated Dirac Delta distribution at point zero. Thus,  $\delta_T(\omega) \rightarrow 0$ ,  $T \rightarrow \infty$ , for  $\omega \neq 0$ , and  $\delta_T(0) \rightarrow \infty$ ,  $T \rightarrow \infty$ . The a.s. upper bound (54) allows to apply Dominated Convergence Theorem in (52). Specifically, from (53) and (54), keeping in mind (55), Dominated Convergence Theorem leads to, for every  $j = 1, \dots, \Gamma(n, d)$ ,  $l = 1, \dots, \Gamma(h, d)$ ,  $n, h \in \mathbb{N}_0$ ,

$$\lim_{T \rightarrow \infty} E \left| X_{n,j,h,l}^{(T)} - X_{n,j,h,l}^{(\infty)} \right|^2 = 2(f_n(0) f_h(0) - f_n(0) f_h(0)) = 0. \tag{56}$$

Note that, in equation (56), we also have applied

$$\int_{[-\pi, \pi]^2} \delta(0 - \omega) \delta(0 - \xi) f_n(\omega) f_h(\xi) d\xi d\omega = f_n(0) f_h(0),$$



since, by Parseval identity, for every  $n \in \mathbb{N}_0$ ,

$$\begin{aligned}
\int_{-\pi}^{\pi} |f_n(\omega)|^2 d\omega &\leq \sum_{n \in \mathbb{N}_0} \Gamma(n, d) \int_{-\pi}^{\pi} |f_n(\omega)|^2 d\omega \\
&= \sum_{t \in \mathbb{Z}} \sum_{n \in \mathbb{N}_0} \sum_{j=1}^{\Gamma(n, d)} \left| \mathcal{R}_t(S_{n, j}^{(d)})(S_{n, j}^{(d)}) \right|^2 \\
&= \sum_{t \in \mathbb{Z}} \|\mathcal{R}_t\|_{\mathcal{S}(L^2(\mathbb{M}_d, d\nu, \mathbb{C}))}^2 \leq \sum_{t \in \mathbb{Z}} \left[ \|\mathcal{R}_t\|_{L^1(L^2(\mathbb{M}_d, d\nu, \mathbb{C}))} \right]^2 \\
&\leq K \sum_{t \in \mathbb{Z}} \|\mathcal{R}_t\|_{L^1(L^2(\mathbb{M}_d, d\nu, \mathbb{C}))} < \infty,
\end{aligned} \tag{57}$$

for certain positive constant  $K$ . The last inequality in (57) follows under  $H_0$ , since  $\sum_{t \in \mathbb{Z}} \|\mathcal{R}_t\|_{L^1(L^2(\mathbb{M}_d, d\nu, \mathbb{C}))} < \infty$ , and, in particular,  $\|\mathcal{R}_t\|_{L^1(L^2(\mathbb{M}_d, d\nu, \mathbb{C}))} \rightarrow 0$ , as  $t \rightarrow \infty$ .

Equation (56) implies, for every  $j = 1, \dots, \Gamma(n, d)$ ,  $l = 1, \dots, \Gamma(h, d)$ ,  $n, h \in \mathbb{N}_0$ , the convergence in the mean-square sense of the entry sequence  $\{X_{n, j, h, l}^{(T)}, T > 0\}$  of a random four-dimensional array sequence  $\{X_{n, j, h, l}^{(T)}, j = 1, \dots, \Gamma(n, d), l = 1, \dots, \Gamma(h, d), n, h \in \mathbb{N}_0; T > 0\}$  to the entry  $X_{n, j, h, l}^{(\infty)}$  of the random array  $\{X_{n, j, h, l}^{(\infty)}, j = 1, \dots, \Gamma(n, d), l = 1, \dots, \Gamma(h, d), n, h \in \mathbb{N}_0\}$ , as  $T \rightarrow \infty$ . Applying again Parseval identity and triangle inequality from equations (28), (47) and (48),

$$E \|X^{(T)} - X^{(\infty)}\|_{\mathcal{S}(L^2(\mathbb{M}_d, d\nu, \mathbb{C}))}^2 \leq 8 \|\mathcal{F}_0\|_{L^1(\mathcal{S}(L^2(\mathbb{M}_d, d\nu, \mathbb{C})))}^2 < \infty,$$

under SRD (see equation (50)). Dominated Convergence Theorem then leads to

$$\begin{aligned}
&\lim_{T \rightarrow \infty} E \|X^{(T)} - X^{(\infty)}\|_{\mathcal{S}(L^2(\mathbb{M}_d, d\nu, \mathbb{C}))}^2 \\
&= \sum_{n, h \in \mathbb{N}_0} \sum_{j=1}^{\Gamma(n, d)} \sum_{l=1}^{\Gamma(h, d)} \lim_{T \rightarrow \infty} E \left| X_{n, j, h, l}^{(T)} - X_{n, j, h, l}^{(\infty)} \right|^2, \\
&+ \sum_{n, h \in \mathbb{N}_0} \sum_{j=1}^{\Gamma(n, d)} \sum_{l=1}^{\Gamma(h, d)} \lim_{T \rightarrow \infty} E \left| \overline{X_{h, l, n, j}^{(T)}} - X_{n, j, h, l}^{(\infty)} \right|^2.
\end{aligned} \tag{58}$$

From equations (56) and (58), the convergence to zero of  $E \|X^{(T)} - X^{(\infty)}\|_{\mathcal{S}(L^2(\mathbb{M}_d, d\nu, \mathbb{C}))}^2$ , as  $T \rightarrow \infty$ , follows. Hence, the convergence in probability, and in distribution sense of  $X^{(T)}$  to  $X^{(\infty)}$  also holds.

## B Proofs for Section 3

### B.1 Proof of Lemma 5

**Proof.** Let us consider

$$\begin{aligned}
& \left\| \int_{-\pi}^{\pi} [\mathcal{F}_{\omega} - \mathcal{F}_{\omega}^{(T)}] d\omega \right\|_{\mathcal{S}(L^2(\mathbb{M}_d, d\nu, \mathbb{C}))}^2 \\
&= \sum_{n \in \mathbb{N}_0} \sum_{j=1}^{\Gamma(n,d)} \int_{[-\pi, \pi]^2} [f_n(\omega) - f_n^{(T)}(\omega)] \overline{f_n(\xi)} d\xi d\omega \\
&+ \int_{[-\pi, \pi]^2} [f_n^{(T)}(\omega) - f_n(\omega)] \overline{f_n^{(T)}(\xi)} d\xi d\omega, \tag{59}
\end{aligned}$$

where the sequence of functions

$$f_n^{(T)}(\omega) = \int_{-\pi}^{\pi} F_T(\omega - \xi) f_n(\xi) d\xi, \quad \forall \omega \in [-\pi, \pi], \quad n \in \mathbb{N}_0,$$

defines the frequency-varying pure point spectra of the operator family  $\left\{ \mathcal{F}_{\omega}^{(T)} = E \left[ \mathcal{P}_{\omega}^{(T)} \right], \omega \in [-\pi, \pi] \right\}$ , for every  $T \geq 2$ .

Since for every  $n \in \mathbb{N}_0$ , under  $H_1$ ,  $f_n(\cdot) \in L^1([-\pi, \pi])$ , applying well-known properties of Féjer kernel, we obtain, as  $T \rightarrow \infty$ ,

$$f_n^{(T)}(\omega) \rightarrow f_n(\omega), \quad \forall \omega \in [-\pi, \pi] \setminus \Lambda_0, \quad \text{with } \int_{\Lambda_0} d\omega = 0. \tag{60}$$

From Young convolution inequality in  $L^2([-\pi, \pi])$ , for each  $n \in \mathbb{N}_0$ , and for every  $T \geq 2$ ,

$$\int_{[-\pi, \pi]} |f_n^{(T)}(\omega)|^2 d\omega \leq \int_{[-\pi, \pi]} |f_n(\omega)|^2 d\omega < \infty, \tag{61}$$

since  $l_{\alpha}, L_{\alpha} \in (0, 1/2)$  under  $H_1$ . Thus,  $f_n^{(T)} \in L^2([-\pi, \pi])$ , for every  $n \in \mathbb{N}_0$ , and  $T$ .

To apply Dominated Convergence Theorem in (59), the following additional inequalities are considered, obtained from triangle inequality, Young convolution inequality for functions in  $L^1([-\pi, \pi])$ , and Jensen's inequality, keeping in mind that  $f_n(\omega) \geq 0$ , a.s. in  $\omega \in [-\pi, \pi]$ , for every  $n \in \mathbb{N}_0$ ,

$$\begin{aligned}
& \left| \int_{[-\pi, \pi]^2} \overline{f_n^{(T)}(\xi)} f_n^{(T)}(\omega) d\xi d\omega \right| \leq \int_{[-\pi, \pi]^2} \left| \overline{f_n^{(T)}(\xi)} f_n^{(T)}(\omega) \right| d\xi d\omega \\
& \leq \int_{[-\pi, \pi]^2} |f_n(\xi) f_n(\omega)| d\xi d\omega = \left[ \int_{[-\pi, \pi]} f_n(\omega) d\omega \right]^2 \leq \int_{[-\pi, \pi]} |f_n(\omega)|^2 d\omega. \tag{62}
\end{aligned}$$

Also, in a similar way,

$$\begin{aligned}
\left| \int_{[-\pi, \pi]^2} \overline{f_n^{(T)}(\xi)} f_n(\omega) d\xi d\omega \right| &\leq \int_{[-\pi, \pi]} |f_n(\omega)|^2 d\omega \\
\left| \int_{[-\pi, \pi]^2} \overline{f_n(\xi)} f_n^{(T)}(\omega) d\xi d\omega \right| &\leq \int_{[-\pi, \pi]} |f_n(\omega)|^2 d\omega \\
\left| \int_{[-\pi, \pi]^2} f_n(\xi) f_n(\omega) d\xi d\omega \right| &\leq \int_{[-\pi, \pi]} |f_n(\omega)|^2 d\omega.
\end{aligned} \tag{63}$$

Under (16),

$$\sum_{n \in \mathbb{N}_0} \Gamma(n, d) \int_{[-\pi, \pi]} |f_n(\omega)|^2 d\omega = \int_{[-\pi, \pi]} \|\mathcal{F}_\omega\|_{\mathcal{S}(L^2(\mathbb{M}_d, d\nu, \mathbb{C}))}^2 d\omega < \infty. \tag{64}$$

From equations (60)–(64), one can apply Dominated Convergence Theorem in equation (59), obtaining

$$\begin{aligned}
&\lim_{T \rightarrow \infty} \left\| \int_{-\pi}^{\pi} [\mathcal{F}_\omega - \mathcal{F}_\omega^{(T)}] d\omega \right\|_{\mathcal{S}(L^2(\mathbb{M}_d, d\nu, \mathbb{C}))}^2 \\
&= \sum_{n \in \mathbb{N}_0} \sum_{j=1}^{\Gamma(n, d)} \int_{[-\pi, \pi]^2} \lim_{T \rightarrow \infty} \overline{f_n^{(T)}(\xi)} [f_n^{(T)}(\omega) - f_n(\omega)] d\xi d\omega \\
&+ \int_{[-\pi, \pi]^2} \lim_{T \rightarrow \infty} \overline{f_n(\xi)} [f_n(\omega) - f_n^{(T)}(\omega)] d\xi d\omega = 0.
\end{aligned} \tag{65}$$

The rate of convergence to zero of the bias is now obtained in the time domain. Let  $B_n$ ,  $n \in \mathbb{N}_0$ , be defined as in equation (55). The function sequence

$$\left\{ \mathbb{I}_{[-(T-1), T-1]}(t) \frac{T - |t|}{T} B_n(t), t \in \mathbb{Z}, n \in \mathbb{N}_0 \right\}_{T \geq 2}$$

pointwise converges to  $B_n(t)$  with rate of convergence  $T^{-1}$ , and satisfies, for every  $T \geq 2$ ,

$$\left| \mathbb{I}_{[-(T-1), T-1]}(t) \frac{T - |t|}{T} B_n(t) \right|^2 \leq |B_n(t)|^2. \tag{66}$$

Under (16), from Parseval identity,

$$\begin{aligned}
\sum_{t \in \mathbb{Z}} \sum_{n \in \mathbb{N}_0} \Gamma(n, d) |B_n(t)|^2 &= \sum_{t \in \mathbb{Z}} \|\mathcal{R}_t\|_{\mathcal{S}(L^2(\mathbb{M}_d, d\nu, \mathbb{C}))}^2 \\
&= \int_{-\pi}^{\pi} \|\mathcal{F}_\omega\|_{\mathcal{S}(L^2(\mathbb{M}_d, d\nu, \mathbb{C}))}^2 d\omega < \infty.
\end{aligned} \tag{67}$$

From equations (66) and (67), Dominated Convergence Theorem then leads to

$$\begin{aligned} & \lim_{T \rightarrow \infty} \sum_{t \in \mathbb{Z}} \left\| \mathcal{R}_t - \mathbb{I}_{[-(T-1), T-1]}(t) \frac{T-|t|}{T} \mathcal{R}_t \right\|_{\mathcal{S}(L^2(\mathbb{M}_d, d\nu, \mathbb{C}))}^2 \\ &= \sum_{t \in \mathbb{Z}} \sum_{n \in \mathbb{N}_0} \Gamma(n, d) \lim_{T \rightarrow \infty} \left| B_n(t) - \mathbb{I}_{[-(T-1), T-1]}(t) \frac{T-|t|}{T} B_n(t) \right|^2 = 0 \end{aligned} \quad (68)$$

and  $\sum_{t \in \mathbb{Z}} \left\| \mathcal{R}_t - \mathbb{I}_{[-(T-1), T-1]}(t) \frac{T-|t|}{T} \mathcal{R}_t \right\|_{\mathcal{S}(L^2(\mathbb{M}_d, d\nu, \mathbb{C}))}^2 = \mathcal{O}(T^{-2})$ . Hence, the desired result follows applying again Parseval identity.

## B.2 Proof of Corollary 1

**Proof.**

For every  $x, y \in \mathbb{M}_d$ , from Lemmas F10 and F12 of Appendix F in the Supplementary Material of [20],

$$\begin{aligned} E[\widehat{f}_\omega^{(T)}(x, y)] &= \left[ \frac{2\pi}{T} \right] \sum_{s=1}^{T-1} W^{(T)} \left( \omega - \frac{2\pi s}{T} \right) f_{\frac{2\pi s}{T}}^{(T)}(x, y) \\ &= \int_{\mathbb{R}} W(\xi) f_{\omega - \xi B_T}^{(T)}(x, y) d\xi + \mathcal{O}(B_T^{-1} T^{-1}). \end{aligned} \quad (69)$$

Applying Lemma 5, from equation (69),

$$\begin{aligned} & \int_{-\pi}^{\pi} E_{H_1}[\widehat{\mathcal{F}}_\omega^{(T)}] d\omega \Big|_{\mathcal{S}(L^2(\mathbb{M}_d, d\nu, \mathbb{C}))} = \int_{-\pi}^{\pi} \left[ \int_{\mathbb{R}} W(\xi) \mathcal{F}_{\omega - \xi B_T}^{(T)} d\xi + \mathcal{O}(B_T^{-1} T^{-1}) \right] d\omega \\ &= \int_{\mathbb{R}} W(\xi) \int_{-\pi}^{\pi} [\mathcal{F}_{\omega - \xi B_T} + \mathcal{O}(T^{-1})] d\omega d\xi + \mathcal{O}(B_T^{-1} T^{-1}) \\ &= \int_{-\pi}^{\pi} \int_{\mathbb{R}} W(\xi) \mathcal{F}_{\omega - \xi B_T} d\xi d\omega + \mathcal{O}(T^{-1}) + \mathcal{O}(B_T^{-1} T^{-1}), \end{aligned} \quad (70)$$

as we wanted to prove.

## B.3 Proof of Lemma 6

**Proof.**

Assumption A1 implies that

$$\text{cum}(X_{t_1}(\tau_1), X_{t_2}(\tau_2), X_{t_3}(\tau_3), X_{t_4}(\tau_4)) \in L^2(\mathbb{M}_d^4, \otimes_{i=1}^4 \nu(dx_i), \mathbb{R}),$$

where  $L^2(\mathbb{M}_d^4, \otimes_{i=1}^4 \nu(dx_i), \mathbb{R}) \equiv \mathcal{S}(L^2(\mathbb{M}_d^2, \otimes_{i=1}^2 \nu(dx_i), \mathbb{R}))$ , with  $\mathcal{S}(L^2(\mathbb{M}_d^2, \otimes_{i=1}^2 \nu(dx_i), \mathbb{R}))$  being the space of Hilbert–Schmidt operators on

$L^2(\mathbb{M}_d^2, \otimes_{i=1}^2 \nu(dx_i), \mathbb{R})$ . Hence, there exists an orthonormal basis  $\{\phi_n, n \in \mathbb{N}\}$  of  $L^2(\mathbb{M}_d^2, \otimes_{i=1}^2 \nu(dx_i), \mathbb{R})$  such that, for every  $n \geq 1$ ,

$$\begin{aligned} & \int_{\mathbb{M}_d} \text{cum}(X_{u_1}, X_{u_2}, X_{u_3}, X_0)(\tau_1, \tau_2, \tau_3, \tau_4) \phi_n(\tau_3, \tau_4) \nu(d\tau_3) \nu(d\tau_4) \\ &= B_n(u_1, u_2, u_3) \phi_n(\tau_1, \tau_2), \quad \forall (\tau_1, \tau_2) \in \mathbb{M}_d \times \mathbb{M}_d. \end{aligned} \quad (71)$$

Furthermore,

$$\begin{aligned} & \int_{[-\pi, \pi]^3} \text{cum}\left(\tilde{X}_{\omega_1}^{(T)}(\tau_1), \tilde{X}_{\omega_2}^{(T)}(\tau_2), \tilde{X}_{\omega_3}^{(T)}(\tau_3), \tilde{X}_{\omega_4}^{(T)}(\tau_4)\right) d\omega_1 d\omega_2 d\omega_3 \\ &= \mathcal{S}(L^2(\mathbb{M}_d^2, \otimes_{i=1}^2 \nu(dx_i), \mathbb{C})) \frac{1}{(2\pi T)^2} \int_{[-\pi, \pi]^3} \sum_{t_1, t_2, t_3, t_4=0}^{T-1} \exp\left(-i \sum_{j=1}^3 (t_j - t_4) \omega_j\right) \\ & \times \exp\left(-it_4 \sum_{j=1}^4 \omega_j\right) \text{cum}(X_{t_1-t_4}(\tau_1), X_{t_2-t_4}(\tau_2), X_{t_3-t_4}(\tau_3), X_0(\tau_4)) \prod_{j=1}^3 d\omega_j \\ &= \mathcal{S}(L^2(\mathbb{M}_d^2, \otimes_{i=1}^2 \nu(dx_i), \mathbb{C})) \int_{[-\pi, \pi]^3} \frac{1}{(2\pi T)^2} \sum_{u_1, u_2, u_3=-(T-1)}^{T-1} \exp\left(-i \sum_{j=1}^3 u_j \omega_j\right) \\ & \times \text{cum}(X_{u_1}(\tau_1), X_{u_2}(\tau_2), X_{u_3}(\tau_3), X_0(\tau_4)) \\ & \times \sum_{t \in \mathbb{Z}} h^{(T)}(u_1 + t) h^{(T)}(u_2 + t) h^{(T)}(u_3 + t) h^{(T)}(t) \exp\left(-it \left(\sum_{j=1}^4 \omega_j\right)\right) \prod_{j=1}^3 d\omega_j, \end{aligned} \quad (72)$$

where  $h(t) = 1, 0 \leq t \leq T$ , and  $h(t) = 0$ , otherwise, and we have considered the change of variable  $u_j = t_j - t_4, j = 1, 2, 3$ .

Denote, for every  $n \geq 1$ , and  $(\omega_1, \omega_2, \omega_3) \in [-\pi, \pi]^3$ ,

$$f_n(\omega_1, \omega_2, \omega_3) = \int_{[-\pi, \pi]^3} \exp\left(-i \sum_{j=1}^3 \omega_j u_j\right) B_n(u_1, u_2, u_3) du_1 du_2 du_3,$$

where  $\{B_n(u_1, u_2, u_3), n \geq 1\}$  satisfies (71). From equations (71)–(72), apply-

ing Fourier transform inversion formula, for each  $n \geq 1$ ,

$$\begin{aligned}
& T \int_{[-\pi, \pi]^3 \times \mathbb{M}_d^4} \text{cum} \left( \tilde{X}_{\omega_1}^{(T)}(\tau_1), \tilde{X}_{\omega_2}^{(T)}(\tau_2), \tilde{X}_{\omega_3}^{(T)}(\tau_3), \tilde{X}_{\omega_4}^{(T)}(\tau_4) \right) \\
& \quad \times \phi_n(\tau_1, \tau_2) \phi_n(\tau_3, \tau_4) \prod_{j=1}^4 d\tau_j \prod_{i=1}^3 d\omega_i \\
&= \frac{1}{(2\pi)^2 T} \int_{[-\pi, \pi]^6} \sum_{u_1, u_2, u_3 = -(T-1)}^{T-1} \exp \left( -i \sum_{j=1}^3 u_j (\omega_j - \xi_j) \right) \\
& \quad \times \sum_{t \in \mathbb{Z}} h^{(T)}(u_1 + t) h^{(T)}(u_2 + t) h^{(T)}(u_3 + t) h^{(T)}(t) \exp \left( -it \left( \sum_{j=1}^4 \omega_j \right) \right) \\
& \quad \quad \times f_n(\xi_1, \xi_2, \xi_3) \prod_{j=1}^3 d\xi_j \prod_{i=1}^3 d\omega_i \\
&= \frac{1}{(2\pi)^2 T} \int_{[-\pi, \pi]^6} \left[ \sum_{u_1, u_2, u_3 = -(T-1)}^{T-1} \exp \left( -i \sum_{j=1}^3 u_j (\omega_j - \xi_j) \right) \right. \\
& \quad \left. \times \sum_{t \in \mathbb{Z}} \exp \left( -it \left( \sum_{j=1}^4 \omega_j \right) \right) h \left( t + \max_{j=1,2,3} |u_j| \right) \right] f_n(\xi_1, \xi_2, \xi_3) \prod_{j=1}^3 d\xi_j \prod_{i=1}^3 d\omega_i
\end{aligned}$$

As  $T \rightarrow \infty$ , uniformly in  $\omega_4 \in [-\pi, \pi]$ ,

$$\begin{aligned}
& \frac{1}{T} \left[ \sum_{u_1, u_2, u_3 = -(T-1)}^{T-1} \exp \left( -i \sum_{j=1}^3 u_j (\omega_j - \xi_j) \right) \right. \\
& \quad \left. \times \sum_{t \in \mathbb{Z}} \exp \left( -it \left( \sum_{j=1}^4 \omega_j \right) \right) h \left( t + \max_{j=1,2,3} |u_j| \right) \right] \rightarrow \delta(\boldsymbol{\omega} - \boldsymbol{\xi}), \quad (74)
\end{aligned}$$

where  $\delta(\boldsymbol{\omega} - \boldsymbol{\xi}) = \prod_{j=1}^3 \delta(\omega_j - \xi_j)$  denotes the Dirac Delta distribution, defining the kernel of the identity operator on  $L^2([-\pi, \pi]^3)$ . Using the notation

$$\begin{aligned}
\delta_T(\boldsymbol{\omega} - \boldsymbol{\xi}) &:= \frac{1}{T} \left[ \sum_{u_1, u_2, u_3 = -(T-1)}^{T-1} \exp \left( -i \sum_{j=1}^3 u_j (\omega_j - \xi_j) \right) \right. \\
& \quad \left. \times \sum_{t \in \mathbb{Z}} \exp \left( -it \left( \sum_{j=1}^4 \omega_j \right) \right) h \left( t + \max_{j=1,2,3} |u_j| \right) \right] \quad (75)
\end{aligned}$$

equation (73) can be rewritten as

$$\begin{aligned}
& T \int_{[-\pi, \pi]^3} \text{cum} \left( \tilde{X}_{\omega_1}^{(T)}(\tau_1), \tilde{X}_{\omega_2}^{(T)}(\tau_2), \tilde{X}_{\omega_3}^{(T)}(\tau_3), \tilde{X}_{\omega_4}^{(T)}(\tau_4) \right) \\
& \quad \times \phi_n(\tau_1, \tau_2) \phi_n(\tau_3, \tau_4) \prod_{j=1}^4 d\tau_j \prod_{i=1}^3 d\omega_i \\
& = \frac{1}{(2\pi)^2} \int_{[-\pi, \pi]^6} \delta_T(\boldsymbol{\omega} - \boldsymbol{\xi}) f_n(\boldsymbol{\xi}) d\boldsymbol{\xi} d\boldsymbol{\omega}, \quad n \geq 1. \tag{76}
\end{aligned}$$

Note that, for  $T \geq T_0$ , with  $T_0$  sufficiently large,

$$|\delta_T(\boldsymbol{\omega} - \boldsymbol{\xi}) f_n(\boldsymbol{\xi})| \leq |f_n(\boldsymbol{\xi})|, \quad \boldsymbol{\omega} \neq \boldsymbol{\xi}, \tag{77}$$

since  $\delta_T(\boldsymbol{\omega} - \boldsymbol{\xi}) \rightarrow 0$ ,  $T \rightarrow \infty$ , for every  $(\boldsymbol{\omega}, \boldsymbol{\xi}) \in [-\pi, \pi]^6 \setminus \Lambda$ , with  $\Lambda = \{(\boldsymbol{\omega}, \boldsymbol{\xi}) \in [-\pi, \pi]^6; \boldsymbol{\omega} = \boldsymbol{\xi}\} \subset [-\pi, \pi]^6$  having zero Lebesgue measure.

Since, under Assumption A1,

$$\begin{aligned}
& \int_{[-\pi, \pi]^3} \sum_{n \geq 1} |f_n(\omega_1, \omega_2, \omega_3)|^2 \prod_{j=1}^3 d\omega_j \\
& = \int_{[-\pi, \pi]^3} \|\mathcal{F}_{\omega_1, \omega_2, \omega_3}\|_{\mathcal{S}(L^2(\mathbb{M}_d^2, \otimes_{i=1}^2 \nu(dx_i), \mathbb{C}))}^2 \prod_{j=1}^3 d\omega_j \\
& = \sum_{t_1, t_2, t_3 \in \mathbb{Z}} \|\text{cum}(X_{t_1}, X_{t_2}, X_{t_3}, X_0)\|_2^2 < \infty, \tag{78}
\end{aligned}$$

the functional upper bound in (77) satisfies

$$\begin{aligned}
& \int_{[-\pi, \pi]^6} \sum_{n \geq 1} |f_n(\omega_1, \omega_2, \omega_3)|^2 \prod_{j=1}^6 d\omega_j \\
& = (2\pi)^3 \int_{[-\pi, \pi]^3} \sum_{n \geq 1} |f_n(\omega_1, \omega_2, \omega_3)|^2 \prod_{j=1}^3 d\omega_j < \infty.
\end{aligned}$$

One can then apply Dominated Convergence Theorem to obtain as  $T \rightarrow \infty$ , uniformly in  $\omega_4 \in [-\pi, \pi]$ ,

$$\left\| \int_{[-\pi, \pi]^3} \left[ T \text{cum} \left( \tilde{X}_{\omega_1}^{(T)}, \tilde{X}_{\omega_2}^{(T)}, \tilde{X}_{\omega_3}^{(T)}, \tilde{X}_{\omega_4}^{(T)} \right) - \mathcal{F}_{\omega_1, \omega_2, \omega_3} \right] \prod_{j=1}^3 d\omega_j \right\|_{\mathcal{S}(L^2(\mathbb{M}_d^2, \otimes_{i=1}^2 \nu(dx_i), \mathbb{C}))} \rightarrow 0,$$

and

$$\begin{aligned} T \int_{[-\pi, \pi]^3} \text{cum} \left( \tilde{X}_{\omega_1}^{(T)}, \tilde{X}_{\omega_2}^{(T)}, \tilde{X}_{\omega_3}^{(T)}, \tilde{X}_{\omega_4}^{(T)} \right) \prod_{i=1}^3 d\omega_i \\ = \int_{[-\pi, \pi]^3} \mathcal{F}_{\omega_1, \omega_2, \omega_3} \prod_{j=1}^3 d\omega_j + \mathcal{O}(T^{-1}), \end{aligned}$$

in the norm of the space  $\mathcal{S}(L^2(\mathbb{M}_d^2, \otimes_{i=1}^2 \nu(dx_i), \mathbb{C}))$  as we wanted to prove.

## C Proofs for Section 4

### C.1 Proof of Proposition 1

**Proof.** From equation (32) in Corollary 1, under  $H_1$  (see equations (9)–(17)), for  $T$  sufficiently large, and for every  $n \in \mathbb{N}_0$ ,

$$\begin{aligned} & \left| \int_{[-\sqrt{B_T}/2, \sqrt{B_T}/2]} E_{H_1}[\hat{f}_n^{(T)}(\omega)] \frac{d\omega}{\sqrt{B_T}} \right| \\ &= \left| \int_{[-\sqrt{B_T}/2, \sqrt{B_T}/2]} \int_{-\pi}^{\pi} \frac{1}{B_T} W\left(\frac{\omega - \alpha}{B_T}\right) f_n(\alpha) d\alpha \frac{d\omega}{\sqrt{B_T}} \right| \\ &+ \mathcal{O}(B_T^{-1}T^{-1}) + \mathcal{O}(T^{-1}) \\ &= \int_{-\pi}^{\pi} \frac{1}{B_T} \left[ \int_{[-\sqrt{B_T}/2, \sqrt{B_T}/2]} W\left(\frac{\omega - \alpha}{B_T}\right) \frac{d\omega}{\sqrt{B_T}} \right] f_n(\alpha) d\alpha \\ &+ \mathcal{O}(B_T^{-1}T^{-1}) + \mathcal{O}(T^{-1}) \\ &\simeq \frac{1}{\sqrt{B_T}} \int_{-\pi}^{\pi} \frac{1}{\sqrt{B_T}} W\left(\frac{-\alpha}{B_T}\right) f_n(\alpha) d\alpha + \mathcal{O}(B_T^{-1}T^{-1}) + \mathcal{O}(T^{-1}) \\ &\geq g(T) = \mathcal{O}(B_T^{-1/2-l_\alpha}), \end{aligned} \tag{79}$$

with  $0 < l_\alpha \leq \alpha(n) \leq L_\alpha < 1/2$ ,  $n \in \mathbb{N}_0$ . Here,  $a_T \simeq b_T$  means that the two sequences have the same limit as  $T \rightarrow \infty$ . From (79), under  $H_1$ ,

$$\begin{aligned} & \left\| \int_{[-\sqrt{B_T}/2, \sqrt{B_T}/2]} E_{H_1}[\hat{\mathcal{F}}_\omega^{(T)}] \frac{d\omega}{\sqrt{B_T}} \right\|_{\mathcal{S}(L^2(\mathbb{M}_d, d\nu, \mathbb{C}))} \\ &\geq \left\| \int_{[-\sqrt{B_T}/2, \sqrt{B_T}/2]} E_{H_1}[\hat{\mathcal{F}}_\omega^{(T)}] \frac{d\omega}{\sqrt{B_T}} \right\|_{\mathcal{L}(L^2(\mathbb{M}_d, d\nu, \mathbb{C}))} \\ &= \sup_{n \in \mathbb{N}_0} \left| \int_{[-\sqrt{B_T}/2, \sqrt{B_T}/2]} \int_{\mathbb{R}} W(\xi) f_n(\omega - \xi B_T) d\xi \frac{d\omega}{\sqrt{B_T}} + \mathcal{O}(B_T^{-1}T^{-1}) + \mathcal{O}(T^{-1}) \right| \\ &\geq g(T) = \mathcal{O}(B_T^{-1/2-l_\alpha}), \quad T \rightarrow \infty, \end{aligned} \tag{80}$$



where  $\mathcal{L}(L^2(\mathbb{M}_d, d\nu, \mathbb{C}))$  denotes the space of bounded linear operators on  $L^2(\mathbb{M}_d, d\nu, \mathbb{C})$ .

## C.2 Proof of Theorem 2

**Proof.** From Lemmas 5 and 6, applying trace formula,

$$\begin{aligned}
& \int_{-\pi}^{\pi} E_{H_1} \left\| \widehat{\mathcal{F}}_{\omega}^{(T)} - E_{H_1}[\widehat{\mathcal{F}}_{\omega}^{(T)}] \right\|_{\mathcal{S}(L^2(\mathbb{M}_d, d\nu, \mathbb{C}))}^2 d\omega \\
&= \frac{2\pi}{T} \int_{-\pi}^{\pi} \sum_{n, h \in \mathbb{N}_0} \sum_{j=1}^{\Gamma(n, d)} \sum_{l=1}^{\Gamma(h, d)} \left| \int_{-\pi}^{\pi} W^{(T)}(\omega - \alpha) W^{(T)}(\omega - \alpha) f_n(\alpha) f_h(\alpha) d\alpha \right| d\omega \\
&+ \frac{2\pi}{T} \int_{-\pi}^{\pi} \sum_{n, h \in \mathbb{N}_0} \sum_{j=1}^{\Gamma(n, d)} \sum_{l=1}^{\Gamma(h, d)} \left| \int_{-\pi}^{\pi} W^{(T)}(\omega - \alpha) W^{(T)}(\omega + \alpha) f_n(\alpha) f_h(\alpha) d\alpha \right| d\omega \\
&+ \mathcal{O}(B_T^{-2} T^{-2}) + \mathcal{O}(T^{-1}) \\
&\leq \frac{2\pi}{TB_T} \sum_{n, h \in \mathbb{N}_0} \sum_{j=1}^{\Gamma(n, d)} \sum_{l=1}^{\Gamma(h, d)} 2 \int_{[-\pi, \pi]} f_n(\omega) f_h(\omega) d\omega + \mathcal{O}(B_T^{-2} T^{-2}) + \mathcal{O}(T^{-1}) \\
&= h(T) = \mathcal{O}(B_T^{-1} T^{-1}), \quad T \rightarrow \infty. \tag{81}
\end{aligned}$$

Note that, equation (81) follows under  $H_1$  from condition (37), since

$$\begin{aligned}
& \sum_{n, h \in \mathbb{N}_0} \sum_{j=1}^{\Gamma(n, d)} \sum_{l=1}^{\Gamma(h, d)} 2 \int_{[-\pi, \pi]} f_n(\omega) f_h(\omega) d\omega \\
&\leq 2 \sum_{n, h \in \mathbb{N}_0} \sum_{j=1}^{\Gamma(n, d)} \sum_{l=1}^{\Gamma(h, d)} \left[ \int_{-\pi}^{-1} + \int_1^{\pi} \right] M_n(\omega) M_h(\omega) d\omega \\
&\quad + \int_{-1}^1 M_n(\omega) M_h(\omega) |\omega|^{-2L\alpha} d\omega = \mathcal{O}(1).
\end{aligned}$$

### C.3 Proof of Corollary 2

**Proof.** Applying triangle and Jensen inequalities, we obtain from Corollary 1 and Theorem 2

$$\begin{aligned}
& \left\| \int_{-\pi}^{\pi} E_{H_1} \left[ \widehat{\mathcal{F}}_{\omega}^{(T)} - \int_{-\pi}^{\pi} W(\xi) \mathcal{F}_{\omega - B_T \xi} d\xi \right] d\omega \right\|_{\mathcal{S}(L^2(\mathbb{M}_d, d\nu, \mathbb{C}))} \\
& \leq \left\| \int_{-\pi}^{\pi} E_{H_1} \left[ \widehat{\mathcal{F}}_{\omega}^{(T)} - E_{H_1} \left[ \widehat{\mathcal{F}}_{\omega}^{(T)} \right] \right] d\omega \right\|_{\mathcal{S}(L^2(\mathbb{M}_d, d\nu, \mathbb{C}))} \\
& \quad + \left\| \int_{-\pi}^{\pi} \left[ E_{H_1} \left[ \widehat{\mathcal{F}}_{\omega}^{(T)} \right] - \int_{-\pi}^{\pi} W(\xi) \mathcal{F}_{\omega - B_T \xi} d\xi \right] d\omega \right\|_{\mathcal{S}(L^2(\mathbb{M}_d, d\nu, \mathbb{C}))} \\
& \leq \left[ \int_{-\pi}^{\pi} E_{H_1} \left\| \widehat{\mathcal{F}}_{\omega}^{(T)} - E_{H_1} \left[ \widehat{\mathcal{F}}_{\omega}^{(T)} \right] \right\|_{\mathcal{S}(L^2(\mathbb{M}_d, d\nu, \mathbb{C}))}^2 d\omega \right]^{1/2} \\
& \quad + \left\| \int_{-\pi}^{\pi} \left[ E_{H_1} \left[ \widehat{\mathcal{F}}_{\omega}^{(T)} \right] - \int_{-\pi}^{\pi} W(\xi) \mathcal{F}_{\omega - B_T \xi} d\xi \right] d\omega \right\|_{\mathcal{S}(L^2(\mathbb{M}_d, d\nu, \mathbb{C}))} \\
& = \mathcal{O}(T^{-1/2} B_T^{-1/2}), \quad T \rightarrow \infty. \tag{82}
\end{aligned}$$

### C.4 Proof of Theorem 3

**Proof.** The proof of this result is inspired in the proof of Theorem 2 of [11] in the time domain for real-valued time series. Specifically, the test statistic operator  $\mathcal{S}_{B_T}$  is rewritten as

$$\begin{aligned}
\mathcal{S}_{B_T} &= \sqrt{B_T T} \int_{[-\sqrt{B_T}/2, \sqrt{B_T}/2]} E_{H_1} \left[ \widehat{\mathcal{F}}_{\omega}^{(T)} \right] \frac{d\omega}{\sqrt{B_T}} \\
& \circ \left[ \mathbb{I}_{L^2(\mathbb{M}_d, d\nu, \mathbb{C})} + \left[ \int_{[-\sqrt{B_T}/2, \sqrt{B_T}/2]} \left( \widehat{\mathcal{F}}_{\omega}^{(T)} - E_{H_1} \left[ \widehat{\mathcal{F}}_{\omega}^{(T)} \right] \right) \frac{d\omega}{\sqrt{B_T}} \right] \right. \\
& \left. \circ \left[ \int_{[-\sqrt{B_T}/2, \sqrt{B_T}/2]} E_{H_1} \left[ \widehat{\mathcal{F}}_{\omega}^{(T)} \right] \frac{d\omega}{\sqrt{B_T}} \right]^{-1} \right], \tag{83}
\end{aligned}$$

where  $\circ$  means composition of operators,  $\mathbb{I}_{L^2(\mathbb{M}_d, d\nu, \mathbb{C})}$  is the identity operator on the space  $L^2(\mathbb{M}_d, d\nu, \mathbb{C})$ , and  $\left[ \int_{[-\sqrt{B_T}/2, \sqrt{B_T}/2]} E_{H_1} \left[ \widehat{\mathcal{F}}_{\omega}^{(T)} \right] \frac{d\omega}{\sqrt{B_T}} \right]^{-1}$  denotes the inverse of operator  $\int_{[-\sqrt{B_T}/2, \sqrt{B_T}/2]} E_{H_1} \left[ \widehat{\mathcal{F}}_{\omega}^{(T)} \right] \frac{d\omega}{\sqrt{B_T}}$ .

Our strategy will be to first prove that operator

$$\sqrt{B_T T} \int_{[-\sqrt{B_T}/2, \sqrt{B_T}/2]} E_{H_1} \left[ \widehat{\mathcal{F}}_{\omega}^{(T)} \right] \frac{d\omega}{\sqrt{B_T}}$$

diverges in the norm of the space  $\mathcal{S}(L^2(\mathbb{M}_d, d\nu, \mathbb{C}))$  under  $H_1$ . Secondly, under the conditions of Theorem 2, we will derive the convergence to zero as  $T \rightarrow \infty$  of random operator

$$\left[ \int_{[-\sqrt{B_T}/2, \sqrt{B_T}/2]} \left[ \widehat{\mathcal{F}}_\omega^{(T)} - E_{H_1} \left[ \widehat{\mathcal{F}}_\omega^{(T)} \right] \right] \frac{d\omega}{\sqrt{B_T}} \right] \circ \left[ \int_{[-\sqrt{B_T}/2, \sqrt{B_T}/2]} E_{H_1} \left[ \widehat{\mathcal{F}}_\omega^{(T)} \right] \frac{d\omega}{\sqrt{B_T}} \right]^{-1},$$

in the space  $\mathcal{L}_{\mathcal{S}(L^2(\mathbb{M}_d, d\nu, \mathbb{C}))}(\Omega, \mathcal{A}, P)$ , which holds with a suitable rate under  $l_\alpha > 1/4$  and  $B_T = T^{-\beta}$ ,  $\beta \in (0, 1)$ , allowing the application of Borell Cantelli Lemma to ensure almost surely convergence. Specifically, from Proposition 1, as  $T \rightarrow \infty$ ,

$$\begin{aligned} & \left\| \sqrt{B_T T} \int_{[-\sqrt{B_T}/2, \sqrt{B_T}/2]} E_{H_1} \left[ \widehat{\mathcal{F}}_\omega^{(T)} \right] \frac{d\omega}{\sqrt{B_T}} \right\|_{\mathcal{S}(L^2(\mathbb{M}_d, d\nu, \mathbb{C}))} \\ & \geq g(T) = \mathcal{O}(T^{1/2} B_T^{-l_\alpha}). \end{aligned} \quad (84)$$

In the second term in (83), the following inequality holds

$$\begin{aligned} & E_{H_1} \left\| \int_{[-\sqrt{B_T}/2, \sqrt{B_T}/2]} \left[ \widehat{\mathcal{F}}_\omega^{(T)} - E_{H_1} \left[ \widehat{\mathcal{F}}_\omega^{(T)} \right] \right] \frac{d\omega}{\sqrt{B_T}} \right. \\ & \quad \left. \circ \left[ \int_{[-\sqrt{B_T}/2, \sqrt{B_T}/2]} E_{H_1} \left[ \widehat{\mathcal{F}}_\omega^{(T)} \right] \frac{d\omega}{\sqrt{B_T}} \right]^{-1} \right\|_{\mathcal{S}(L^2(\mathbb{M}_d, d\nu, \mathbb{C}))}^2 \\ & \leq \left\| \left[ \int_{[-\sqrt{B_T}/2, \sqrt{B_T}/2]} E_{H_1} \left[ \widehat{\mathcal{F}}_\omega^{(T)} \right] \frac{d\omega}{\sqrt{B_T}} \right]^{-1} \right\|_{\mathcal{L}(L^2(\mathbb{M}_d, d\nu, \mathbb{C}))}^2 \\ & \quad \times E_{H_1} \left\| \int_{[-\sqrt{B_T}/2, \sqrt{B_T}/2]} \left[ \widehat{\mathcal{F}}_\omega^{(T)} - E_{H_1} \left[ \widehat{\mathcal{F}}_\omega^{(T)} \right] \right] \frac{d\omega}{\sqrt{B_T}} \right\|_{\mathcal{S}(L^2(\mathbb{M}_d, d\nu, \mathbb{C}))}^2 \end{aligned} \quad (85)$$

From equation (80),

$$\begin{aligned} & \left\| \left[ \int_{[-\sqrt{B_T}/2, \sqrt{B_T}/2]} E_{H_1} \left[ \widehat{\mathcal{F}}_\omega^{(T)} \right] \frac{d\omega}{\sqrt{B_T}} \right]^{-1} \right\|_{\mathcal{L}(L^2(\mathbb{M}_d, d\nu, \mathbb{C}))}^2 \\ & \leq b(T) = \mathcal{O}(B_T^{2l_\alpha+1}), \quad T \rightarrow \infty, \end{aligned} \quad (86)$$

and, from Theorem 2,

$$\begin{aligned}
& \int_{[-\sqrt{B_T}/2, \sqrt{B_T}/2]} \text{Var}_{H_1} \left( \widehat{\mathcal{F}}_\omega^{(T)} \right) \frac{d\omega}{\sqrt{B_T}} \\
& \leq \int_{[-\pi, \pi]} \text{Var}_{H_1} \left( \widehat{\mathcal{F}}_\omega^{(T)} \right) \frac{d\omega}{\sqrt{B_T}} \leq u(T) = \mathcal{O}(T^{-1} B_T^{-1-1/2}), \quad T \rightarrow \infty.
\end{aligned} \tag{87}$$

For each  $T \geq 2$ , applying Jensen inequality, in terms of the uniform probability measure on the interval  $[-\sqrt{B_T}/2, \sqrt{B_T}/2]$ ,

$$\begin{aligned}
& E_{H_1} \left\| \int_{[-\sqrt{B_T}/2, \sqrt{B_T}/2]} \left[ \widehat{\mathcal{F}}_\omega^{(T)} - E_{H_1} \left[ \widehat{\mathcal{F}}_\omega^{(T)} \right] \right] \frac{d\omega}{\sqrt{B_T}} \right\|_{\mathcal{S}(L^2(\mathbb{M}_d, d\nu, \mathbb{C}))}^2 \\
& = \left\| \int_{[-\sqrt{B_T}/2, \sqrt{B_T}/2]} \left[ \widehat{\mathcal{F}}_\omega^{(T)} - E_{H_1} \left[ \widehat{\mathcal{F}}_\omega^{(T)} \right] \right] \frac{d\omega}{\sqrt{B_T}} \right\|_{\mathcal{L}_{\mathcal{S}(L^2(\mathbb{M}_d, d\nu, \mathbb{C}))}(\Omega, \mathcal{A}, P)}^2 \\
& = \varphi_{H_1} \left( E_{\mathcal{U}([- \sqrt{B_T}/2, \sqrt{B_T}/2])} \left[ \widehat{\mathcal{F}}_\omega^{(T)} - E_{H_1} \left[ \widehat{\mathcal{F}}_\omega^{(T)} \right] \right] \right) \\
& \leq E_{\mathcal{U}([- \sqrt{B_T}/2, \sqrt{B_T}/2])} \left[ \varphi_{H_1} \left( \left[ \widehat{\mathcal{F}}_\omega^{(T)} - E_{H_1} \left[ \widehat{\mathcal{F}}_\omega^{(T)} \right] \right] \right) \right] \\
& = \int_{[-\sqrt{B_T}/2, \sqrt{B_T}/2]} E_{H_1} \left\| \widehat{\mathcal{F}}_\omega^{(T)} - E_{H_1} \left[ \widehat{\mathcal{F}}_\omega^{(T)} \right] \right\|_{\mathcal{S}(L^2(\mathbb{M}_d, d\nu, \mathbb{C}))}^2 \frac{d\omega}{\sqrt{B_T}}, \tag{88}
\end{aligned}$$

where  $E_{\mathcal{U}([- \sqrt{B_T}/2, \sqrt{B_T}/2])}$  denotes expectation under the uniform probability measure on the interval  $[-\sqrt{B_T}/2, \sqrt{B_T}/2]$ , and  $\varphi_{H_1}(\cdot) = \|\cdot\|_{\mathcal{L}_{\mathcal{S}(L^2(\mathbb{M}_d, d\nu, \mathbb{C}))}(\Omega, \mathcal{A}, P)}^2 = E_{H_1} \|\cdot\|_{\mathcal{S}(L^2(\mathbb{M}_d, d\nu, \mathbb{C}))}^2$  is a convex function. Thus, from equations (85)–(88),

$$\begin{aligned}
& E_{H_1} \left\| \int_{[-\sqrt{B_T}/2, \sqrt{B_T}/2]} \left[ \widehat{\mathcal{F}}_\omega^{(T)} - E_{H_1} \left[ \widehat{\mathcal{F}}_\omega^{(T)} \right] \right] \frac{d\omega}{\sqrt{B_T}} \right. \\
& \quad \left. \circ \left[ \int_{[-\sqrt{B_T}/2, \sqrt{B_T}/2]} E_{H_1} \left[ \widehat{\mathcal{F}}_\omega^{(T)} \right] \frac{d\omega}{\sqrt{B_T}} \right]^{-1} \right\|_{\mathcal{S}(L^2(\mathbb{M}_d, d\nu, \mathbb{C}))}^2 \\
& \leq h(T) = \mathcal{O}(T^{-1} B_T^{2l_\alpha - 1/2}), \quad T \rightarrow \infty. \tag{89}
\end{aligned}$$

From equation (89), applying Chebyshev's inequality,

$$\begin{aligned}
& P \left[ \left\| \int_{[-\sqrt{B_T}/2, \sqrt{B_T}/2]} \left[ \widehat{\mathcal{F}}_\omega^{(T)} - E_{H_1} \left[ \widehat{\mathcal{F}}_\omega^{(T)} \right] \right] \frac{d\omega}{\sqrt{B_T}} \right. \right. \\
& \quad \left. \left. \circ \left[ \int_{[-\sqrt{B_T}/2, \sqrt{B_T}/2]} E_{H_1} \left[ \widehat{\mathcal{F}}_\omega^{(T)} \right] \frac{d\omega}{\sqrt{B_T}} \right]^{-1} \right\|_{\mathcal{S}(L^2(\mathbb{M}_d, d\nu, \mathbb{C}))} > \varepsilon \right] \\
& \leq E_{H_1} \left\| \int_{[-\sqrt{B_T}/2, \sqrt{B_T}/2]} \left[ \widehat{\mathcal{F}}_\omega^{(T)} - E_{H_1} \left[ \widehat{\mathcal{F}}_\omega^{(T)} \right] \right] \frac{d\omega}{\sqrt{B_T}} \right. \\
& \quad \left. \circ \left[ \int_{[-\sqrt{B_T}/2, \sqrt{B_T}/2]} E_{H_1} \left[ \widehat{\mathcal{F}}_\omega^{(T)} \right] \frac{d\omega}{\sqrt{B_T}} \right]^{-1} \right\|_{\mathcal{S}(L^2(\mathbb{M}_d, d\nu, \mathbb{C}))}^2 / \varepsilon^2 \\
& \leq h(T) / \varepsilon^2 = \mathcal{O}(T^{-1} B_T^{2l_\alpha - 1/2}). \tag{90}
\end{aligned}$$

Since  $l_\alpha > 1/4$ , hence,  $2l_\alpha - 1/2 = \rho > 0$ , and, for  $B_T = T^{-\beta}$ ,  $T^{-1} B_T^{2l_\alpha - 1/2} = T^{-1-\beta\rho}$ , with  $\beta \in (0, 1)$ , and  $\rho \in (0, 1/2)$ . From equation (90), Borel–Cantelli lemma then leads to, as  $T \rightarrow \infty$ ,

$$\begin{aligned}
& \left\| \int_{[-\sqrt{B_T}/2, \sqrt{B_T}/2]} \left[ \widehat{\mathcal{F}}_\omega^{(T)} - E_{H_1} \left[ \widehat{\mathcal{F}}_\omega^{(T)} \right] \right] \frac{d\omega}{\sqrt{B_T}} \right. \\
& \quad \left. \circ \left[ \int_{[-\sqrt{B_T}/2, \sqrt{B_T}/2]} E_{H_1} \left[ \widehat{\mathcal{F}}_\omega^{(T)} \right] \frac{d\omega}{\sqrt{B_T}} \right]^{-1} \right\|_{\mathcal{S}(L^2(\mathbb{M}_d, d\nu, \mathbb{C}))} \xrightarrow{a.s.} 0. \tag{91}
\end{aligned}$$

The a.s. divergence of  $\|\mathcal{S}_{B_T}\|_{\mathcal{S}(L^2(\mathbb{M}_d, d\nu, \mathbb{C}))}$ , as  $T \rightarrow \infty$ , follows from equations (83), (84) and (91).

## D Figures of Sections 5.2 and 5.3

This appendix contains the figures of Sections 5.2 and 5.3.

### D.1 Examples

The figures below display the generated realizations of multifractionally integrated SPHARMA (1,1) processes, the eigenvalues of LRD operator  $\mathcal{A}$  involved in the multifractional integration operators considered, and the sample values of  $\mathcal{S}_{B_T}$  projected into  $\mathcal{H}_n \otimes \mathcal{H}_n$ ,  $n = 1, \dots, 8$ , for large values of  $T$ .

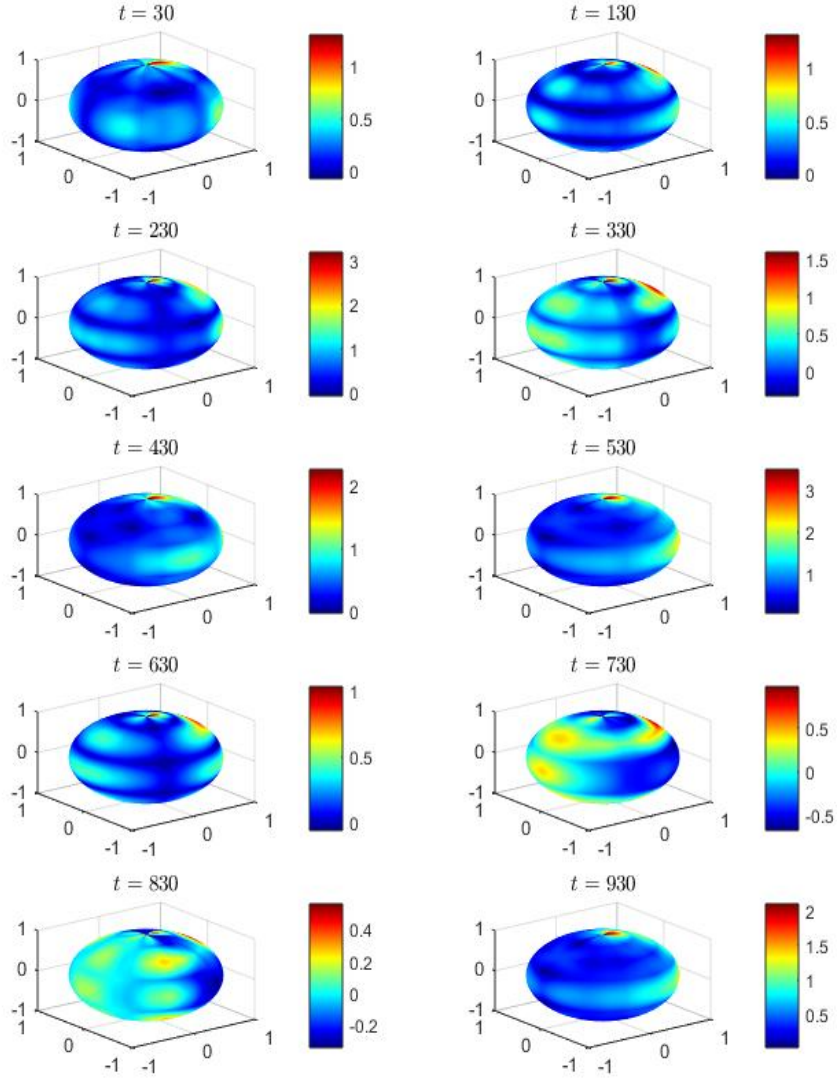


Figure 5: *Example 1.* One sample realization at times  $t = 30, 130, 230, 330, 430, 530, 630, 730, 830, 930$  of multifractally integrated SPHARMA(1,1) process projected into  $\bigoplus_{n=1}^8 \mathcal{H}_n$ , with LRD operator eigenvalues displayed in Figure 6

### D.1.1 Example 1

Figure 5 displays one sample realization of the generated multifractionally integrated SPHARMA (1,1) process projected into  $\bigoplus_{n=1}^8 \mathcal{H}_n$ . Here,  $\lambda_n(\varphi_1) = 0.7 \left(\frac{n+1}{n}\right)^{-3/2}$  and  $\lambda_n(\psi_1) = (0.4) \left(\frac{n+1}{n}\right)^{-5/1.95}$ ,  $n \in \mathbb{N}_0$ . Multifractional integration is given in terms of the eigenvalues  $\alpha(n)$ ,  $n = 1, 2, 3, 4, 5, 6, 7, 8$ , of LRD operator  $\mathcal{A}$ , which are plotted in Figure 6, with  $L_\alpha = 0.4733$ , and  $l_\alpha = 0.2678$ , and  $\alpha(n) = l_\alpha = 0.2678$ ,  $n \geq 9$ . The a.s. divergence in the Hilbert–Schmidt operator norm of  $\mathcal{S}_{B_T}$ , for  $B_T = T^{-1/4}$ , projected into  $\mathcal{H}_n \otimes \mathcal{H}_n$ ,  $n = 1, \dots, 8$ , is illustrated in Figure 7.

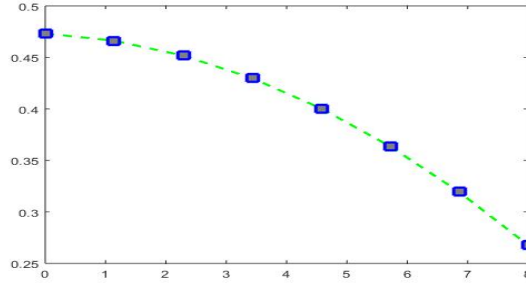


Figure 6: *Example 1.* Eigenvalues  $\alpha(n)$ ,  $n = 1, 2, 3, 4, 5, 6, 7, 8$ , of LRD operator  $\mathcal{A}$ ,  $L_\alpha = 0.4733$ , and  $l_\alpha = 0.2678$

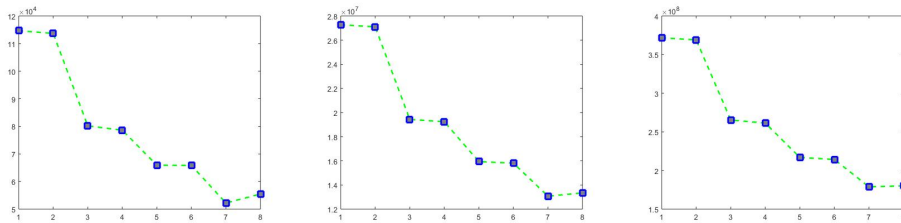


Figure 7: *Example 1.* Sample values of the test operator statistics  $\mathcal{S}_{B_T}$ ,  $B_T = T^{-1/4}$ , projected into  $\mathcal{H}_n \otimes \mathcal{H}_n$ ,  $n = 1, \dots, 8$ ,  $L_\alpha = 0.4733$ , and  $l_\alpha = 0.2678$ , for functional sample sizes  $T = 1000, 10000, 30000$

### D.1.2 Example 2

Figure 8 displays one sample realization of the generated multifractionally integrated SPHARMA (1,1) process projected into  $\bigoplus_{n=1}^8 \mathcal{H}_n$ , with  $\lambda_n(\varphi_1) = 0.7 \left(\frac{n+1}{n}\right)^{-3/2}$  and  $\lambda_n(\psi_1) = (0.4) \left(\frac{n+1}{n}\right)^{-5/1.95}$ ,  $n \in \mathbb{N}_0$ . Multifractional integration is given in terms of the eigenvalues of  $\alpha(n)$ ,  $n = 1, 2, 3, 4, 5, 6, 7, 8$ , of LRD

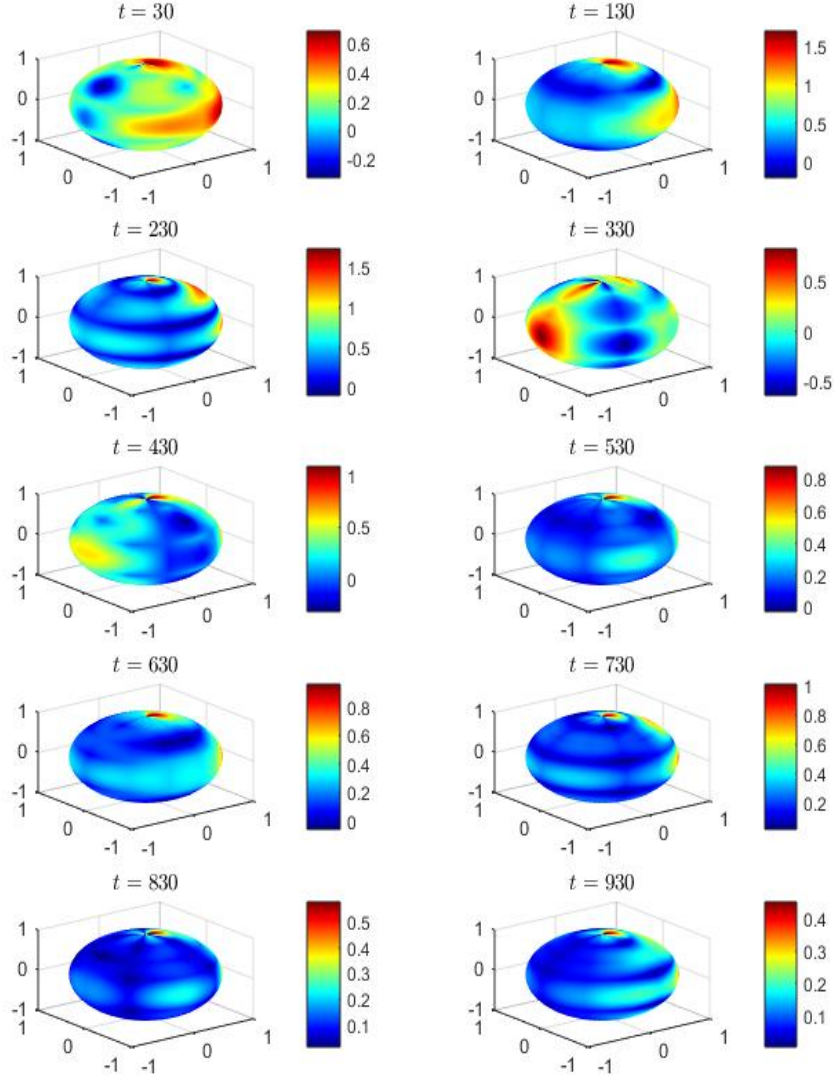


Figure 8: *Example 2.* One sample realization at times  $t = 30, 130, 230, 330, 430, 530, 630, 730, 830, 930$  of multifractally integrated SPHARMA(1,1) process projected into  $\bigoplus_{n=1}^8 \mathcal{H}_n$ , with LRD operator eigenvalues displayed in Figure 9

operator  $\mathcal{A}$ , which are plotted in Figure 9, being  $L_\alpha = 0.3327$ , and  $l_\alpha = 0.2550$ , with  $\alpha(n) = l_\alpha = 0.2550$ ,  $n \geq 9$ . The a.s. divergence in the Hilbert–Schmidt operator norm of  $\mathcal{S}_{B_T}$ , for  $B_T = T^{-1/4}$ , projected into  $\mathcal{H}_n \otimes \mathcal{H}_n$ ,  $n = 1, \dots, 8$ ,



is illustrated in Figure 10.

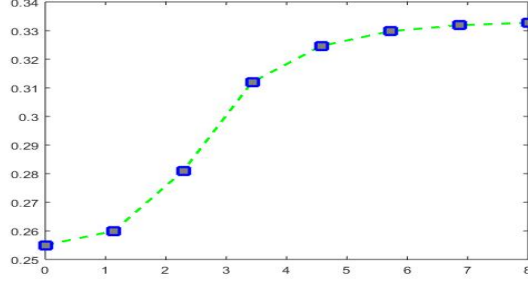


Figure 9: *Example 2.* Eigenvalues  $\alpha(n)$ ,  $n = 1, 2, 3, 4, 5, 6, 7, 8$ , of LRD operator  $\mathcal{A}$ ,  $L_\alpha = 0.3327$ , and  $l_\alpha = 0.2550$

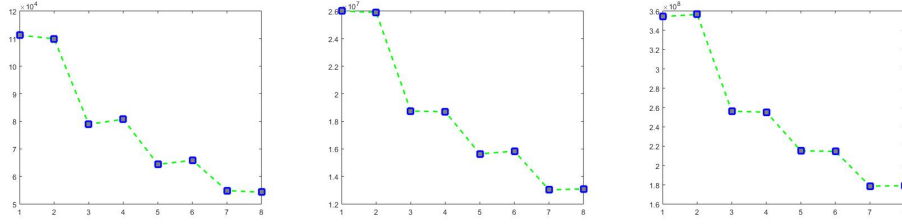


Figure 10: *Example 2.* Sample values of the kernel of the test operator statistics  $\mathcal{S}_{B_T}$ ,  $B_T = T^{-1/4}$ , projected into  $\mathcal{H}_n \otimes \mathcal{H}_n$ ,  $n = 1, \dots, 8$ ,  $L_\alpha = 0.3327$ , and  $l_\alpha = 0.2550$ , for functional sample sizes  $T = 1000, 10000, 30000$

### D.1.3 Example 3

Figure 11 displays one sample realization of the generated multifractionally integrated SPHARMA (1,1) process projected into  $\bigoplus_{n=1}^8 \mathcal{H}_n$ , with  $\lambda_n(\varphi_1) = 0.7 \left(\frac{n+1}{n}\right)^{-3/2}$  and  $\lambda_n(\psi_1) = (0.4) \left(\frac{n+1}{n}\right)^{-5/1.95}$ ,  $n \in \mathbb{N}_0$ . The eigenvalues  $\alpha(n)$ ,  $n = 1, 2, 3, 4, 5, 6, 7, 8$ , of LRD operator  $\mathcal{A}$  are plotted in Figure 12, being  $L_\alpha = 0.4000$ , and  $l_\alpha = 0.2753 = \alpha(n)$ ,  $n \geq 9$ . The a.s. divergence in the Hilbert–Schmidt operator norm of  $\mathcal{S}_{B_T}$ , for  $B_T = T^{-1/4}$ , projected into  $\mathcal{H}_n \otimes \mathcal{H}_n$ ,  $n = 1, \dots, 8$ , is illustrated in Figure 13.

### D.1.4 Example 4

Figure 14 displays one sample realization of the generated multifractionally integrated SPHARMA (1,1) process projected into  $\bigoplus_{n=1}^8 \mathcal{H}_n$ , with  $\lambda_n(\varphi_1) =$

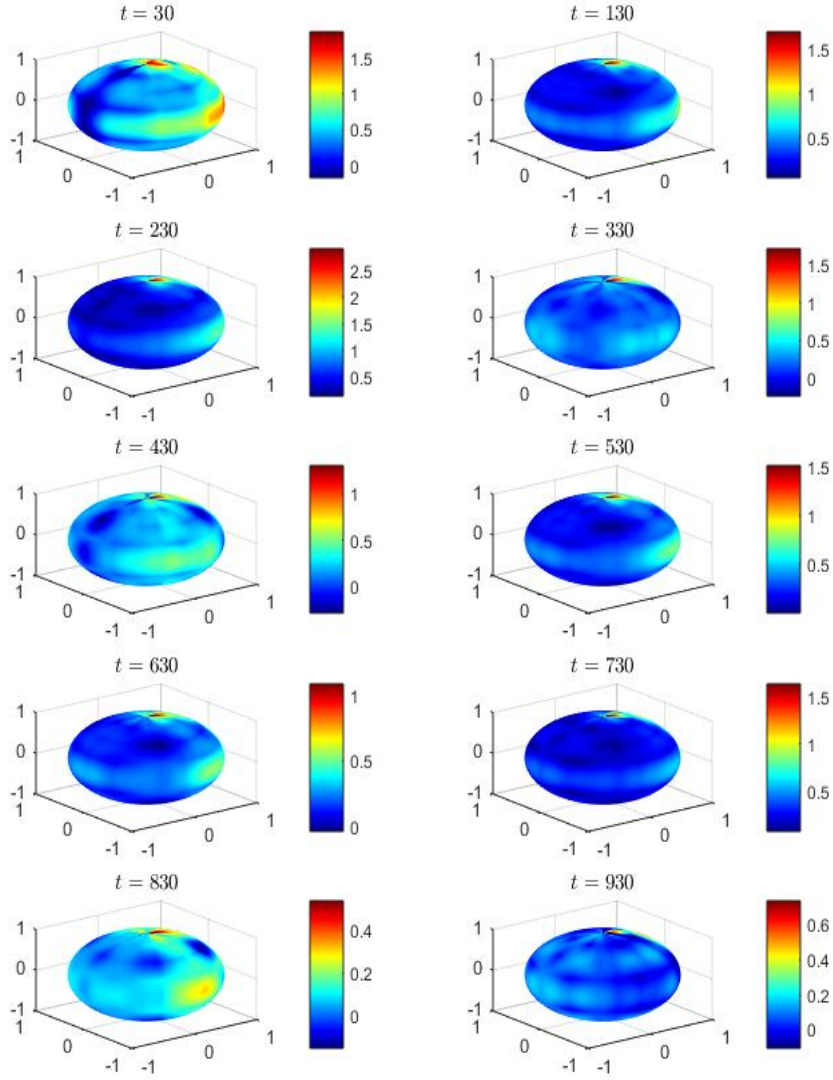


Figure 11: *Example 3.* One sample realization at times  $t = 30, 130, 230, 330, 430, 530, 630, 730, 830, 930$  of multifractionally integrated SPHARMA(1,1) process projected into  $\bigoplus_{n=1}^8 \mathcal{H}_n$ , with LRD operator eigenvalues displayed in Figure 12

$0.7 \left(\frac{n+1}{n}\right)^{-3/2}$  and  $\lambda_n(\psi_1) = (0.4) \left(\frac{n+1}{n}\right)^{-5/1.95}$ ,  $n \in \mathbb{N}_0$ . Multifractional integration is given in terms of the eigenvalues  $\alpha(n)$ ,  $n = 1, 2, 3, 4, 5, 6, 7, 8$ , of LRD operator  $\mathcal{A}$ , plotted in Figure 15, being  $L_\alpha = 0.9982$  and  $l_\alpha = 0.3041$ . The

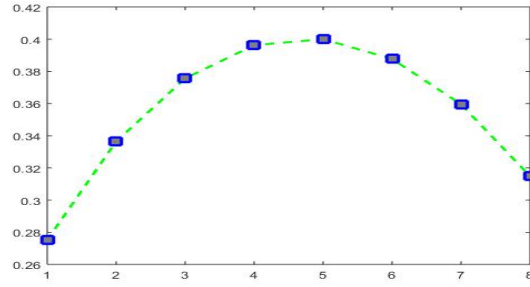


Figure 12: *Example 3.* Eigenvalues  $\alpha(n)$ ,  $n = 1, 2, 3, 4, 5, 6, 7, 8$ , of the LRD operator  $\mathcal{A}$ ,  $L_\alpha = 0.4000$ , and  $l_\alpha = 0.2753$

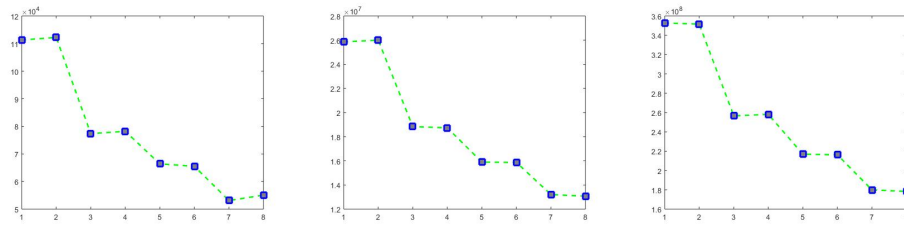


Figure 13: *Example 3.* Sample values of the kernel of the test operator statistics  $\mathcal{S}_{B_T}$ ,  $B_T = T^{-1/4}$ , projected into  $\mathcal{H}_n \otimes \mathcal{H}_n$ ,  $n = 1, \dots, 8$ ,  $L_\alpha = 0.4000$ , and  $l_\alpha = 0.2753$ , for functional sample sizes  $T = 1000, 10000, 30000$

sample values of  $\mathcal{S}_{B_T}$ , for  $B_T = T^{-1/4}$ , projected into  $\mathcal{H}_n \otimes \mathcal{H}_n$ ,  $n = 1, \dots, 8$ , are given in Figure 16.

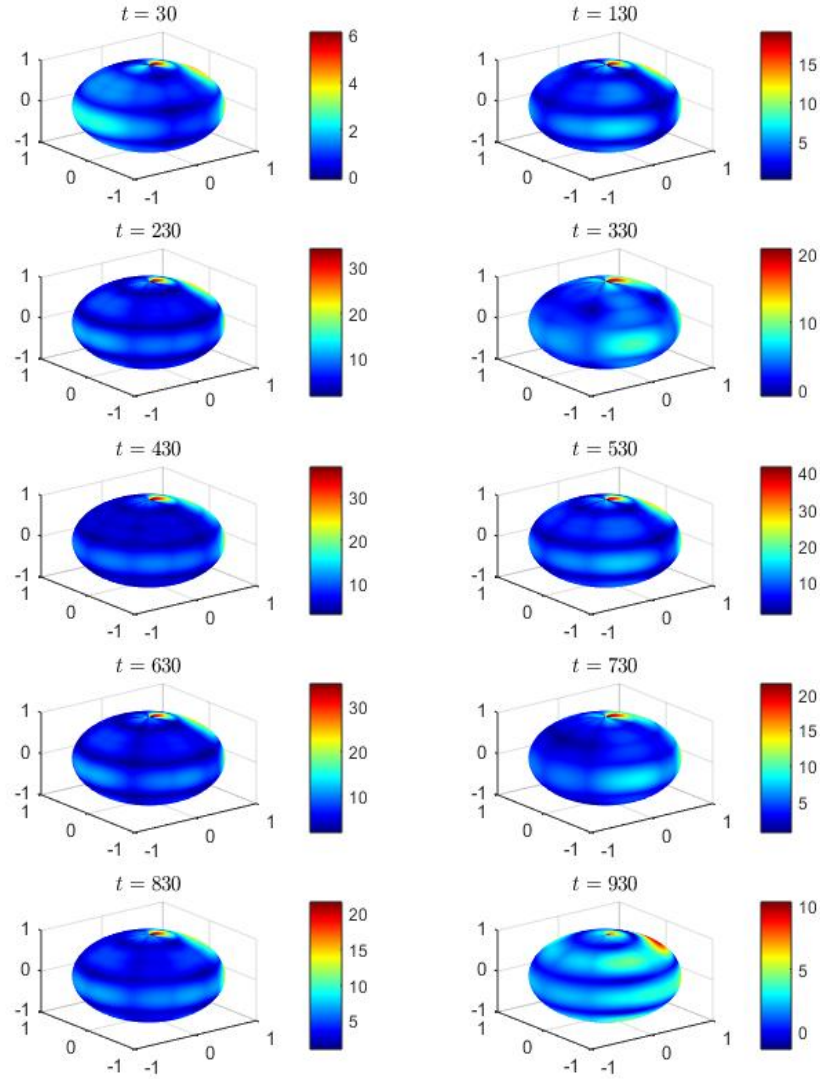


Figure 14: *Example 4*. One sample realization at times  $t = 30, 130, 230, 330, 430, 530, 630, 730, 830, 930$  of multifractally integrated SPHARMA(1,1) process projected into  $\bigoplus_{n=1}^8 \mathcal{H}_n$ , with LRD operator eigenvalues displayed in Figure 15

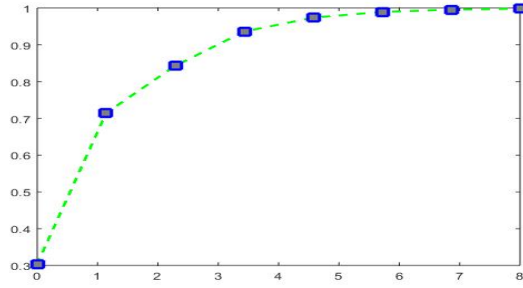


Figure 15: *Example 4.* Eigenvalues  $\alpha(n)$ ,  $n = 1, 2, 3, 4, 5, 6, 7, 8$ , of LRD operator  $\mathcal{A}$ ,  $L_\alpha = 0.9982$  and  $l_\alpha = 0.3041$

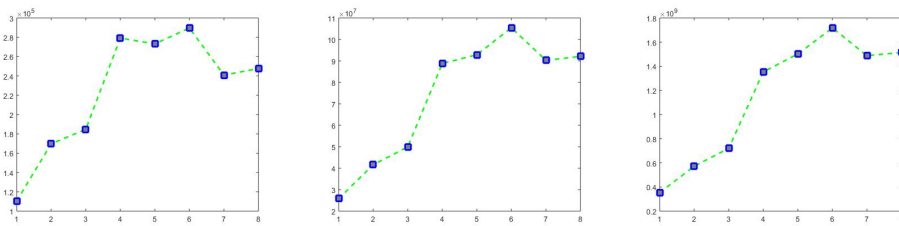


Figure 16: *Example 4.* Sample values of the kernel of the test operator statistics  $\mathcal{S}_{B_T}$ , for  $B_T = T^{-1/4}$ , projected into  $\mathcal{H}_n \otimes \mathcal{H}_n$ ,  $n = 1, \dots, 8$ , with eigenvalues of LRD operator  $\mathcal{A}$  plotted in Figure 15,  $L_\alpha = 0.9982$  and  $l_\alpha = 0.3041$ , for the functional sample sizes  $T = 1000, 10000, 30000$  and

## References

- [1] BERAN, J. (2017). *Mathematical Foundations of Time Series Analysis*. Springer, Switzerland.
- [2] CAPONERA, A. (2021). SPHARMA approximations for stationary functional time series in the sphere. *Stat Infer Stoch Proc* **24** 609–634.
- [3] CAPONERA, A. and MARINUCCI, D. (2021). Asymptotics for spherical functional autoregressions. *Ann Stat* **49** 346–369.
- [4] CHARACIEJUS, V. and RÄCKAUSKAS, A. (2014). Operator self-similar processes and functional central limit theorems. *Stochastic Process. Appl.* **124** 2605–2627.
- [5] CUESTA-ALBERTOS, J.A., FRAIMAN, R. and RANSFORD, T. (2007). A sharp form of the Cramér–Wold theorem. *J. Theoret. Probab.* **20** 201–209.
- [6] DA PRATO, G. and ZABCZYK, J. (2002). *Second Order Partial Differential Equations in Hilbert Spaces*. Cambridge, London.
- [7] DAUTRAY, R. and LIONS, J.L. (1985). *Mathematical Analysis and Numerical Methods for Science and Technology*. Volume **3**: *Spectral Theory and Applications*. Springer, New York.
- [8] DÜKER, M. (2018). Limit theorems for Hilbert space-valued linear processes under long range dependence. *Stochastic Processes and Their Applications* **128** 1439–1465.
- [9] DÜKER, M. (2020). Sample autocovariance operators of long-range dependent Hilbert space-valued linear processes. <https://www.researchgate.net/publication/344364182>.
- [10] GELFAND, I. M. and VILENKIN, N. Y. (1964). *Generalized Functions*, Vol. 4. Academic Press, New York.
- [11] HARRIS, D., MCCABE, B. and LEYBOURNE, S. (2008). Testing for long memory. *Econometric Theory* **24** 143–175.
- [12] KARTSIOUKAS, R., STOEV, R. S. and HSING, T. (2023). Spectral density estimation of function-valued spatial processes. arXiv:2302.02247.
- [13] LI, D., ROBINSON, P.M. and SHANG, H.L. (2019). Long-range dependent curve time series. *J. of the American Statistical Association* **115** 957–971.

- [14] MA, C. and MALYARENKO, A. (2020). Time varying isotropic vector random fields on compact two points homogeneous spaces. *J Theor Probab.* **33** 319–339.
- [15] MARINUCCI, D. and PECCATI, G. (2011). *Random fields on the Sphere. Representation, Limit Theorems and Cosmological Applications*. Mathematical Society Lecture Note Series 389. Cambridge University Press, London.
- [16] MARINUCCI, D., ROSSI, M. and VIDOTTO, A. (2020). Non-universal fluctuations of the empirical measure for isotropic stationary fields on  $\mathbb{S}^2 \times \mathbb{R}$ . *Ann Appl Probab.* **31** 2311–2349.
- [17] MARINUCCI, D., ROSSI, M. and WIGMAN, I. (2020). The asymptotic equivalence of the sample trispectrum and the nodal length for random spherical harmonics. *Ann. Inst. Henri Poincaré Probab. Stat.* **56** 374–390.
- [18] OVALLE–MUÑOZ, D.P. and RUIZ–MEDINA, M.D. (2024a). LRD spectral analysis of multifractional functional time series on manifolds. *TEST* **33** 564–588.
- [19] OVALLE–MUÑOZ, D.P. and RUIZ–MEDINA, M.D. (2024b). Climate change analysis from LRD manifold functional regression. arXiv.5699574.
- [20] PANARETOS, V. M. and TAVAKOLI, S. (2013a). Fourier analysis of stationary time series in function space. *Ann. Statist.* **41** 568–603.
- [21] PANARETOS, V. M. and TAVAKOLI, S. (2013b). Cramér–Karhunen-Loève representation and harmonic principal component analysis of functional time series. *Stochastic Process and their Applications* **123** 2779–2807.
- [22] PHAM, T. and PANARETOS, V. (2018). Methodology and convergence rates for functional time series regression. *Statistica Sinica.* **28** 2521–2539.
- [23] RACKAUSKAS, A. and SUQUET, CH. (2010). On limit theorems for Banach-space-valued linear processes. *Lithuanian Mathematical J.* **50** 71–87.
- [24] RACKAUSKAS, A. and SUQUET, CH. (2011). Operator fractional brownian motion as limit of polygonal lines processes in Hilbert space. *Stochastics and Dynamics* **11** 49–70.
- [25] RAMM, A.G. (2005). *Random Fields Estimation*. Longman Scientific & Technical, England.

- [26] RUBÍN, T. and PANARETOS, V. M. (2020a). Functional lagged regression with sparse noisy observations. *Journal of Time Series Analysis*. **41** 858–882.
- [27] RUBÍN, T. and PANARETOS, V. M. (2020b). Spectral simulation of functional time series. *arXiv preprint arXiv:2007.08458*.
- [28] RUIZ–MEDINA, M. D. (2022). Spectral analysis of long range dependence functional time series. *Fractional Calculus and Applied Analysis* **25** 1426–1458.
- [29] SHAH, I., MUBASSIR, P., ALI, S. and ALBALAWI, O. (2024). A functional autoregressive approach for modeling and forecasting short-term air temperature. *Environ. Sci.* **12** <https://doi.org/10.3389/fenvs.2024.1411237>.
- [30] TAVAKOLI, S. (2014). *Fourier Analysis of Functional Time Series with Applications to DNA Dynamics*. Ph.D. dissertation, EPFL. Available at <http://dx.doi.org/10.5075/epfl-thesis-6320>.
- [31] TAVAKOLI, S. and PANARETOS, V. M. (2016). Detecting and localizing differences in functional time series dynamics: a case study in molecular biophysics. *Journal of the American Statistical Association* **111** 1020–1035.
- [32] TIRELLI, I., MENDEZ, M.A., IANIRO, A. and DISCETTI, S. (2024). A meshless method to compute the proper orthogonal decomposition and its variants from scattered data. *ArXiv* 2407.03173.
- [33] WU, Y., HUANG, CH. and SRIVASTAVA, A. (2024). Shape based functional data analysis. *TEST* **33** 1–47.
- [34] YARGER, D., STOEV, S. and HSING, T. (2022). A functional-data approach to the Argo data. *Ann. Appl. Stat.* **16** 216–246.
- [35] ZHOU, H., LI, L. and ZHU, H. (2013). Tensor regression with applications in neuroimaging data analysis. *J Am Stat Assoc* **108** 540–552.
- [36] ZHU, H., CHEN, Y., IBRAHIM, J. G., LI, Y., HALL, C. and LIN, W. (2009). Intrinsic regression models for positive-definite matrices with applications to diffusion tensor imaging. *J Am Stat Assoc* **104** 1203–1212.